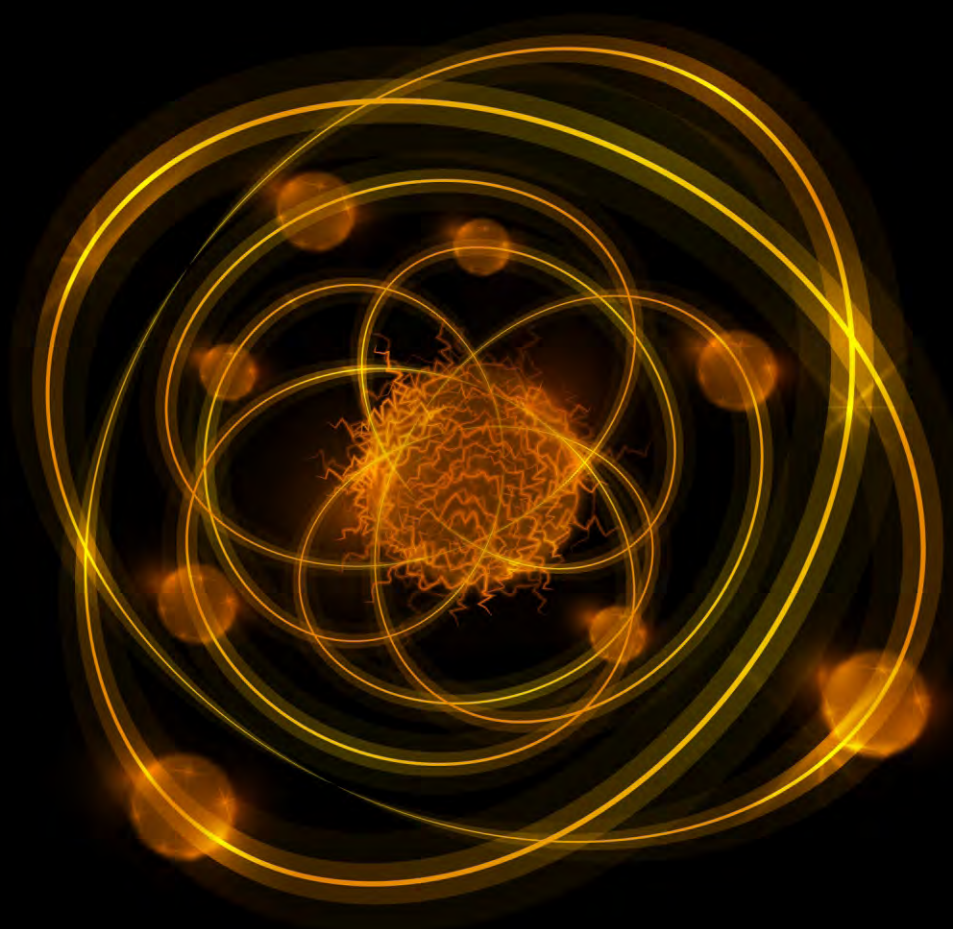


ISSN: 2161-6795

Volume 9, Number 4, October 2019



# World Journal of Nuclear Science and Technology



<https://www.scirp.org/journal/wjnst>

# Journal Editorial Board

ISSN 2161-6795 (Print) ISSN 2161-6809 (Online)

<https://www.scirp.org/journal/wjnst>

---

## Editor-in-Chief

**Prof. Andrzej Grzegorz Chmielewski**

Institute of Nuclear Chemistry and  
Technology, Poland

## Editorial Board

**Dr. Abdullah Aydin**

Kirikkale University, Turkey

**Prof. Jiejun Cai**

Sun Yat-sen University, China

**Prof. Ahmet Cengiz**

Uluda University, Turkey

**Prof. Abdelmajid Choukri**

University of Ibn Tofail, Morocco

**Prof. Snezana Dragovic**

University of Belgrade, Serbia

**Prof. Hardy Christian Ekberg**

Chalmers University of Technology, Sweden

**Prof. Juan-Luis François**

National Autonomous University of Mexico, Mexico

**Prof. Shilun Guo**

China Institute of Atomic Energy, China

**Prof. Shaban Ramadan Mohamed Harb**

South Valley University, Egypt

**Prof. Xiaolin Hou**

Technical University of Denmark, Denmark

**Prof. Ning Liu**

Sichuan University, China

**Prof. Man Gyun Na**

Chosun University, South Korea

**Prof. Dragoslav Nikezic**

University of Kragujevac, Serbia

**Dr. Rafael Rodríguez Pérez**

University of Las Palmas de Gran Canaria, Spain

**Prof. K. Indira Priyadarsini**

Bhabha Atomic Research Centre, India

**Prof. Massimo Rogante**

Studio d'Ingegneria Rogante, Italy

**Prof. Vitalii D. Rusov**

Odessa National Polytechnic University, Ukraine

**Dr. Chhanda Samanta**

Virginia Military Institute, USA

**Prof. Kune Y. Suh**

Seoul National University, South Korea

**Prof. Wenxi Tian**

Xi'an Jiaotong University, China

**Dr. Heiko Timmers**

The University of New South Wales, Australia

**Prof. Marco Túllio Menna Barreto de Vilhena**

Federal University of Rio Grande do Sul, Brazil

**Dr. Jun Wang**

University of Wisconsin Madison, USA

**Dr. Leopoldo A. Pando Zayas**

University of Michigan, USA

# Table of Contents

**Volume 9    Number 4**

**October 2019**

**Diagnostic Reference Level in Frontal Chest X-Ray in Western Côte d'Ivoire**

I. Konate, G. A. Monnehan, D. B. L. H. Gogon, T. P. A. Dali, A. A. Koua, K. Djagouri.....147

**Evaluation of Dosimetric Performance and Global Uncertainty of the Harshaw 6600 Plus System Used to Staff Monitoring in Côte d'Ivoire**

O. Kouakou, G. A. Monnehan, G. B. D. L. Huberson.....159

**Qualification of the ANET Code for Spallation Neutron Yield and Core Criticality in the KUCA ADS**

X. Thalia, P. Savva, M. Varvayanni, J. Maillard, J. Silva, M.-T. Jaekel, N. Catsaros.....174

# World Journal of Nuclear Science and Technology (WJNST)

## Journal Information

### SUBSCRIPTIONS

The *World Journal of Nuclear Science and Technology* (Online at Scientific Research Publishing, <https://www.scirp.org/>) is published quarterly by Scientific Research Publishing, Inc., USA.

#### **Subscription rates:**

Print: \$79 per issue.

To subscribe, please contact Journals Subscriptions Department, E-mail: [sub@scirp.org](mailto:sub@scirp.org)

### SERVICES

#### **Advertisements**

Advertisement Sales Department, E-mail: [service@scirp.org](mailto:service@scirp.org)

#### **Reprints (minimum quantity 100 copies)**

Reprints Co-ordinator, Scientific Research Publishing, Inc., USA.

E-mail: [sub@scirp.org](mailto:sub@scirp.org)

### COPYRIGHT

#### **Copyright and reuse rights for the front matter of the journal:**

Copyright © 2019 by Scientific Research Publishing Inc.

This work is licensed under the Creative Commons Attribution International License (CC BY).

<http://creativecommons.org/licenses/by/4.0/>

#### **Copyright for individual papers of the journal:**

Copyright © 2019 by author(s) and Scientific Research Publishing Inc.

#### **Reuse rights for individual papers:**

Note: At SCIRP authors can choose between CC BY and CC BY-NC. Please consult each paper for its reuse rights.

#### **Disclaimer of liability**

Statements and opinions expressed in the articles and communications are those of the individual contributors and not the statements and opinion of Scientific Research Publishing, Inc. We assume no responsibility or liability for any damage or injury to persons or property arising out of the use of any materials, instructions, methods or ideas contained herein. We expressly disclaim any implied warranties of merchantability or fitness for a particular purpose. If expert assistance is required, the services of a competent professional person should be sought.

### PRODUCTION INFORMATION

For manuscripts that have been accepted for publication, please contact:

E-mail: [wjnst@scirp.org](mailto:wjnst@scirp.org)

# Diagnostic Reference Level in Frontal Chest X-Ray in Western Côte d'Ivoire

Issa Konate<sup>1</sup>, George A. Monnehan<sup>1,2\*</sup>, Douo B. L. H. Gogon<sup>1,2</sup>, Tekpo P. A. Dali<sup>1</sup>, Aka A. Koua<sup>1,2</sup>, Koudou Djagouri<sup>3</sup>

<sup>1</sup>Laboratory of Nuclear Physics and Radiation Protection, Training and Research Unit, Sciences of Matter and Technology, Félix Houphouët-Boigny University, Abidjan, Côte d'Ivoire

<sup>2</sup>Radiation Protection and Nuclear Security Authority, Abidjan, Côte d'Ivoire

<sup>3</sup>High Normal School, Abidjan, Côte d'Ivoire

Email: k\_iss a66@yahoo.fr

**How to cite this paper:** Konate, I., Monnehan, G.A., Gogon, D.B.L.H., Dali, T.P.A., Koua, A.A. and Djagouri, K. (2019) Diagnostic Reference Level in Frontal Chest X-Ray in Western Côte d'Ivoire. *World Journal of Nuclear Science and Technology*, 9, 147-158.

<https://doi.org/10.4236/wjnst.2019.94011>

**Received:** August 8, 2019

**Accepted:** September 6, 2019

**Published:** September 9, 2019

Copyright © 2019 by author(s) and Scientific Research Publishing Inc. This work is licensed under the Creative Commons Attribution International License (CC BY 4.0).

<http://creativecommons.org/licenses/by/4.0/>



Open Access

## Abstract

Our study aims to determine diagnostic reference levels (DRL) for chest front examination in postero anterior (PA) for optimizing patient entrance surface dose (ESD) and dose-area product (DAP) of patients in west of Côte d'Ivoire. 90 patients from three hospitals undergoing conventional radiology were considered. The ESD and DAP for each patient were obtained during chest radiography (PA) examination. The measurements were performed with the device call Dose-Area Product-meter (DAP-meter) with brand Diamentor M4-KDK, type 11017. The DRL were obtained in applying the 75th percentile statistical method to the obtained ESD and DAP. The obtained DRL in ESD for chest radiography for all rooms is 0.40 mGy and in DAP is 54.85 cGy·cm<sup>2</sup>. Our DRL for ESD is higher than those obtained in Abidjan District and in other countries like UK and Cameroon. Our DRL for DAP is higher than those from Abidjan and all other countries for which a similar study was made. The comparison of these values to those from Abidjan and other countries, shows us that radiology technicians can make efforts to choose radiological parameters to reduce ESD. They must use convenable the X-rays tube to reduce DAP by reducing the patient exposure surface.

## Keywords

Conventional Radiology, Entrance Surface-Dose, Dose-Area-Product, Dose-Area Product-Meter, Diagnostic Reference Levels

## 1. Introduction

The excessive variability of doses delivered to patients of the same body size,

during the same examination for the same medical purpose led the International Commission for Radiological Protection (ICRP) to make recommendations in 1996 [1]. The goal is to determine the Diagnostic Reference Levels (DRLs) for the most-performed and most-irradiating examinations to optimize the dose and dose-area product in conventional radiology received by the patient. From then on, many states have transposed the ICRP recommendations into their laws. Today the determination of the DRL is part of the technical cooperation project of the International Atomic Energy Agency (IAEA), n° RAF 9059 [2]. It is within this framework that we are inscribing our work to determine the DRL in western Côte d'Ivoire for three (3) radiology rooms for frontal chest examination for 90 patients. The final objective is to provide conventional radiology practitioners with some reference dose values in order to ensure the management of the doses delivered and the efficient control of the exposure of patients in Côte d'Ivoire. Our work was conducted on patients with a measuring device called DAP-meter. In Côte d'Ivoire, Issa Konaté *et al.* have published in the same conditions two DRLs studies, one on Abidjan frontal chest (PA) examinations [3] and the other on Abidjan lumbar spine examinations [4]. It is worth noting that a preliminary work was conducted by Monnehan *et al.* [5] using a phantom (water-filled can) and TLD dosimeters. The reading of the dose at the entrance was made from a Harshaw 4500 reader.

For this work, we described the material, then the results were presented, then the discussions and conclusion closed our presentation.

## 2. Materials and Methods

### 2.1. Sampling Methods

Three (3) conventional radiology rooms corresponding to 3 hospitals, all located in three (3) cities of western Côte d'Ivoire, were selected. These are the Regional Hospital Center (CHR) in Daloa, the Regional Hospital Center (CHR) in San Pedro, and the General Hospital (HG) in Bangolo. All these rooms comply with the Ivorian standards of at least 25 m<sup>2</sup> of base area and a ceiling height of at least 3.5 m [6] and have been inspected by the competent body. In each of the rooms, we took into account in our measurements, 30 patients [7], all equipped with a bulletin for the examination of the frontal chest and all, 18 years old at least. It should be noted that the examination of the frontal chest is the examination most practiced in these rooms. We excluded from our study patients on bed or chair. In total for our study we had 90 patients.

### 2.2. Data Collection

Our study began after we received permission from each of the managers of the 3 radiology centers. During the months of May, June, July 2016, we went every day to these centers, one after the other. For each patient in our study, we measured the Dose in air (Dair) and dose-area product (DAP) using a DAP-meter. All of these values were recorded on a data collection sheet along with the age,

mass, size, and thickness of the patient portion to be examined. We also noted technical parameters such as source-skin distance, voltage and electrical charge.

### 2.3. Materials

In a conventional radiology room, we have equipment such as the X-ray generator, X-ray tube, desk, wall stand and X-ray viewer. For our study, we brought with us in each room, a DAP-meter brand Diamentor M4-KDK and type 11,017 manufactured by the German company PTW. This device has been previously calibrated by the PTW-Freiburg calibration laboratory. It consists of an ionization chamber and an electrometer connected by two cords. The ionization chamber is placed at the exit of the tube at the collimator and the electrometer is placed at the desk behind the screen. When the beam passes through the ionization chamber, it deposits energy that is transferred by the leads to the electrometer. At this level, this energy is transformed into to dose in air ( $D_{air}$ ) and DAP [8].

### 2.4. Methods for Determining DRLs

We obtained the Entrance Surface Dose ( $ESD$ ) for each patient, from the  $D_{air}$  by the following equation:

$$ESD = D_{air} \times BSF \quad (1)$$

where  $D_{air}$  is the dose in air

( $BSF$  = backscattering factor) with  $BSF = 1.35$  for voltage values included between 60 and 80 kV or 1.5 above 80 kV [9].

We determined the Diagnostic Reference Levels (DRLs) for each examination according to the 75th percentile statistical method in accordance with the recommendations of the European Commission. This is to take as DRL the value of the 75th percentile of  $ESD$  or  $DAP$  for a given exam on a large number of patients and on a large number of  $ESD$  and  $DAP$  values. This is a method used in statistics to remove the limit values from the sample. The 75th percentile of  $n$  values in ascending order is the value of rank  $k$ , given by the following mathematical equation:

$$k = \frac{75n}{100} \quad (2)$$

[10]; where  $n$  is the number of patient.

## 3. Results

### 3.1. Determination of the DRL for the ESD per Center for the Examination of the Frontal Chest (PA)

On this **Figure 1**, we have the values of DRL in  $ESD$  for the examination of the frontal chest in postero-anterior incidence. The highest value of  $ESD$  is obtained at the CHR of Daloa (0.425 mGy) and the lowest is obtained at the CHR of San-Pédro (0.141 mGy).

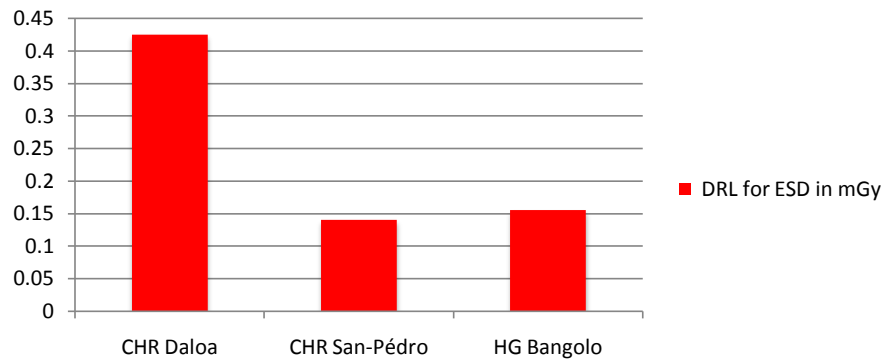


**Figure 1.** Comparison of DRLs values in mGy.

### 3.2. Comparison of Voltage Values in kV and Electrical Charge in mAs of the Rooms of Our Study for the Examination of the Frontal Thorax (AP)

It is observed on **Figure 2**, that the highest mean value of 117.2 kV of the voltage is obtained at HG Bangolo and the lowest average value 81.66 kV is obtained at the CHR of Daloa.

On **Figure 3**, the higher mean value of the electrical charge is obtained at the CHR of Daloa and the lowest is obtained at HG Bangolo.

### 3.3. Determination of the DRL for the DAP per Center for the Examination of the Frontal Chest (PA)

On **Figure 4**, DAP have their highest value obtained at CHR of Daloa (74.02 cGy·cm<sup>2</sup>) and the lowest value obtained at Bangolo HG (15.2 cGy·cm<sup>2</sup>).

### 3.4. Characteristics of the X-Ray Tubes in Each of the Radiology Rooms of Our Study

In **Table 1**, the higher filtration of the tube is observed at the CHR San-Pédro (2 mm Al) and the lowest is obtained at CHR Daloa and HG Bangolo (1 mm Al). The tube at CHR Daloa is almost the same age as that of HG Bangolo. However that of CHR San-Pédro is older than four (4) years. All these devices arrived new in the corresponding radiology rooms.

### 3.5. Voltage in kV and Electrical Charge in mAs, DRLs in mGy and in cGy·cm<sup>2</sup> for All the Centers of Our Study for the Examination of the Frontal Thorax

We calculated the mean tension and the average electrical charge (arithmetic mean) [11]. We have adopted the following notations: average (minimum, maximum) in kV and mAs. Finally, we determined the DRL (75th percentile) in ESD and DAP. The values are shown in **Table 2**.

In **Table 2**, we have reported the mean values of voltages and mAs with their corresponding intervals. We also reported the DRLs values in ESD (0.40 mGy) and in DAP (54.85 cGy·cm<sup>2</sup>) of all 3 rooms in our study.

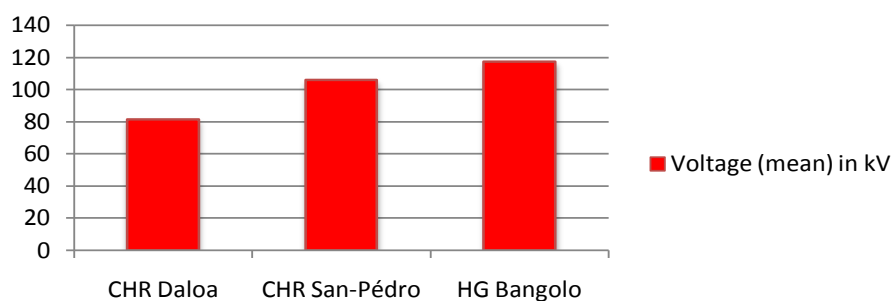


**Figure 2.** Comparison of voltage mean [11] values.

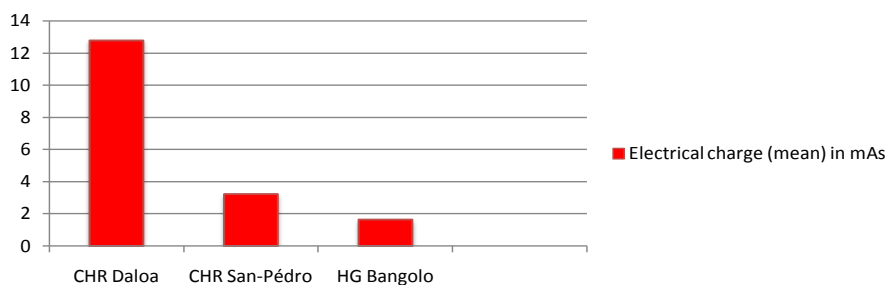


**Figure 3.** Comparison of electrical charge mean [11] values.

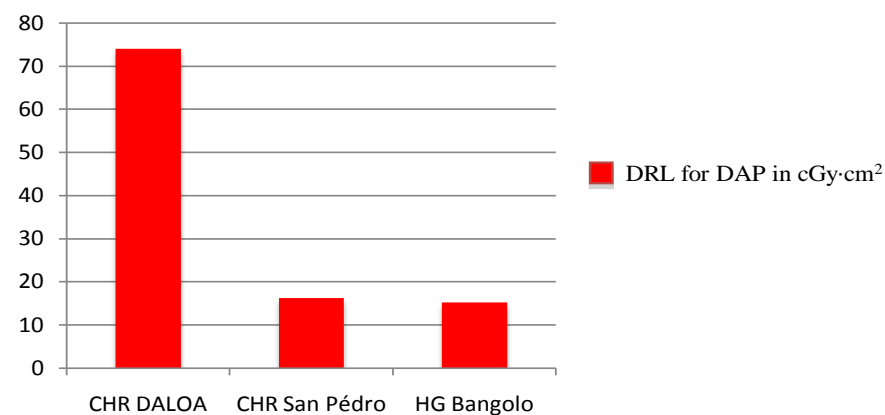


**Figure 4.** Comparison of DRL values in cGy·cm².

**Table 1.** Comparison of age and total filtration of X-ray tubes in our radiology rooms.

Hospital centers	X-ray tubes model	X-ray tubes year of installation	X-ray tubes total filtration
CHR DALOA	Dongmum	2011	1 mm Al
CHR SAN-PEDRO	Toshiba	2015	2 mm Al
HG BANGOLO	Dongmum	2012	1 mm Al

**Table 2.** Exposure parameters with mean values and range (in bracket) and DRL of ESD and DAP for all the hospital centers of our study.

Examination	Voltage (kV)	mAs	DRL	
			ESD (mGy)	DAP (cGy·cm²)
Frontal chest (PA)	101.6 (80 - 122)	6 (1.3 - 16)	0.40	54.85

### 3.6. DRL of Our Study and DRL Obtained in the District of Abidjan for the Examination of the Frontal Thorax (PA) [3]

On **Figure 5**, we observe that the DRL for ESD in our study in the west of Côte d'Ivoire is higher than the one of Abidjan.

On **Figure 6**, the voltage use in Abidjan for the frontal chest exam is higher than the one of our study.

On **Figure 7**, the electrical charge use in Abidjan for the frontal chest exam is smaller than the one use in our study in western Côte d'Ivoire.

We observe on **Figure 8**, that the DRL for DAP in our study in the west of Côte d'Ivoire is higher than the one of Abidjan.

### 3.7. DRL from Our Study and DRL Obtained in Other Countries

On **Figure 9**, we compare the DRL in ESD of our study with those obtained in other countries and institutions outside Africa. Our value 0.40 mGy is close to that of Iran and IAEA [12] [13] but larger than all other values in the figure [14].

On **Figure 10**, we can compare our value of DRL for ESD with those obtained in other African countries. Our DRL value in ESD is equal to that of Nigeria [15], close to that of Cameroon [16] and higher than all other values [17] [18].

On **Figure 11**, which presents the comparison of the DRL for DAP obtained in our study with those of IRNS and other countries outside Africa, the smallest value is obtained in the United Kingdom (UK), 10 cGy·cm<sup>2</sup> [14], and the most large, 54.85 cGy·cm<sup>2</sup> in our study [19] [20].

## 4. Discussion

According to the results of our study, for the examination of the frontal chest, we note that the highest DRL value in ESD of these radiology centers is obtained at CHR Daloa, it is 0.425 mGy. The lowest DRL value is obtained at CHR San-Pédro, 0.141 mGy (**Figure 1**). We explain this situation by the fact that the average value of the voltage used at the CHR Daloa, 81.66 kV is the smallest

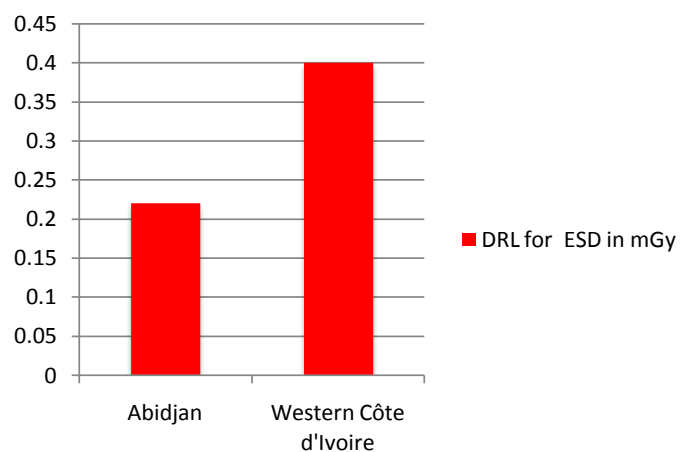


**Figure 5.** Comparison of the DRL for ESD of our study to the one of Abidjan.

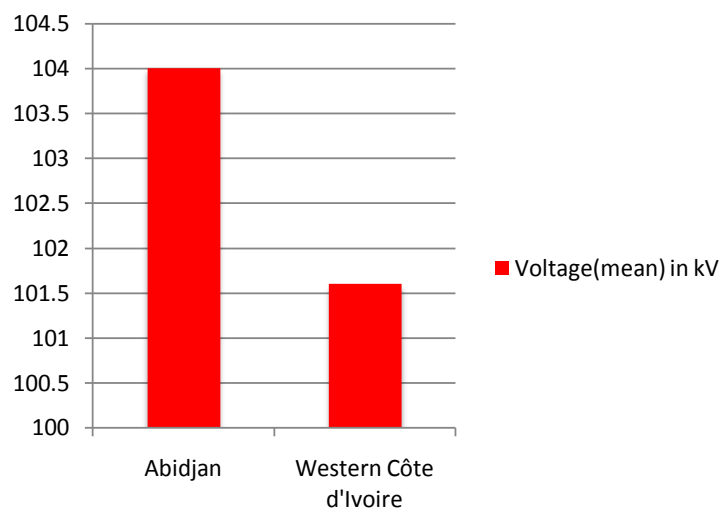


**Figure 6.** Comparison of the voltage to the one of Abidjan.

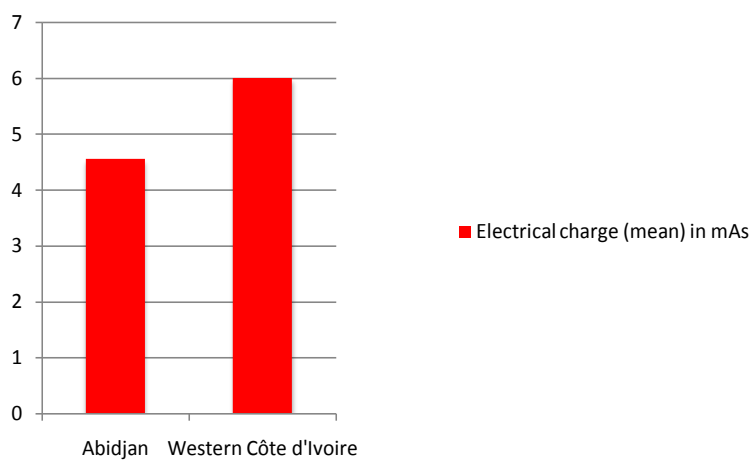


**Figure 7.** Comparison of the electrical charge to the one of Abidjan.

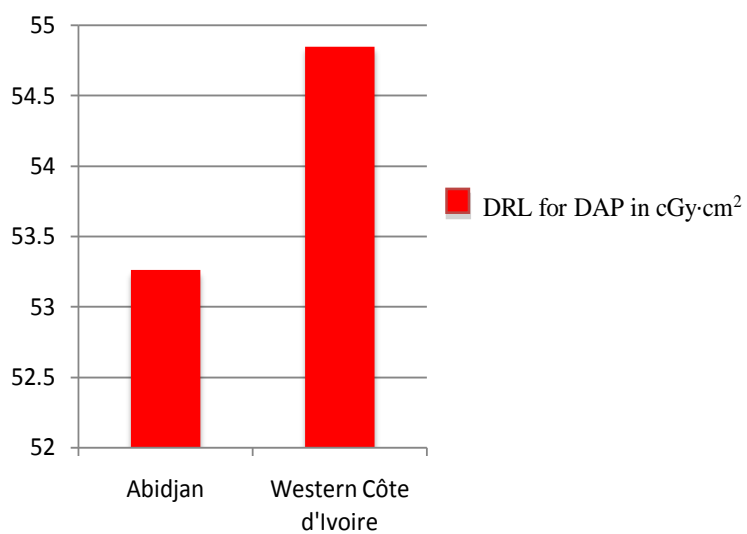


**Figure 8.** Comparison of the DRL for DAP of our study to the one of Abidjan.

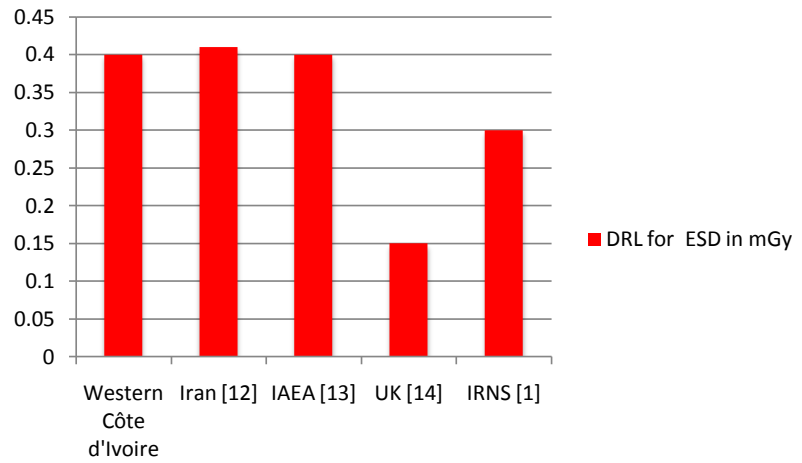


**Figure 9.** Comparison of DRL for ESD obtained in our study with those obtained in other countries and institutions.

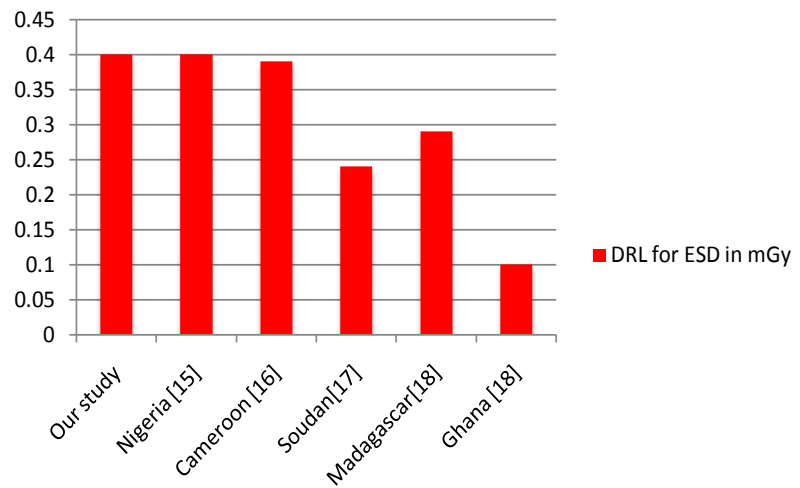


**Figure 10.** Comparison of DRL for ESD obtained in our study with those obtained in other African countries.

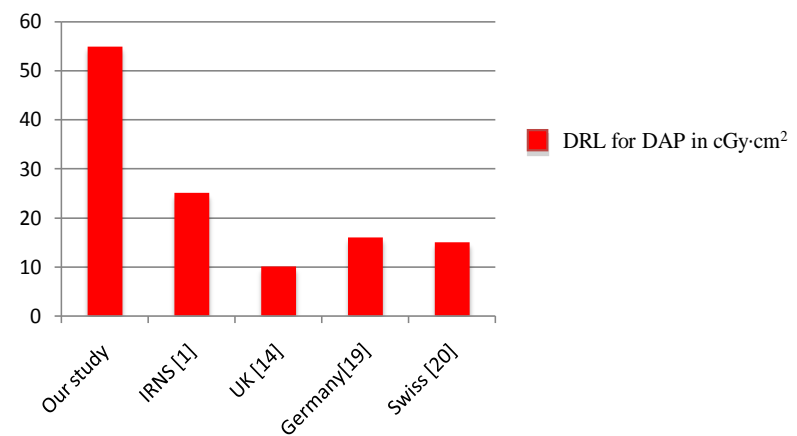


**Figure 11.** Comparison of DRL for DAP obtained in our study with those obtained in other countries.

value compared to other centers (**Figure 2**) and the average value of the electrical charge used in this center, 12.8 mAs, is the largest (**Figure 3**). Indeed, the lower the voltage and the electrical charge, the dose received by the patient is high. According to the French Society of Radiology (FSR) [21], the recommended average voltage is 125 kV in a voltage range (115 - 140) kV and the recommended charging interval is (1.5 - 3) mAs for the examination of the frontal chest with a tendency to increase the tension and decrease the electrical charge. But in our work, the electrical charge is 4 times the maximum value of the recommended interval (1.5 - 3) mAs. The DRL of ESD at CHR San-Pédro is 0.141 mGy. This value is slightly lower than that obtained at Bangolo HG which is 0.156 mGy. It is noted that the average value of the voltage at San Pedro is slightly lower than that of Bangolo's general hospital and that the average electrical charge at San Pedro is slightly larger than at Bangolo's General Hospital, which can be explained by through filtration (**Table 1**). Indeed the filtration of the X-ray tube lowers the dose at the entrance of a patient. The greater the filtration, the lower the dose at entry [22]. FSR recommends total filtration greater than or equal to 3 mm Al. The tube of the CHR of San-Pédro has a total filtration of 2 mm Al while that of HG of Bangolo has a total filtration of 1 mm Al. For DRL in PDS, the highest value is obtained at the CHR of Daloa (74.02 cGy·cm<sup>2</sup>) (**Figure 4**), which is explained by the DRL in ESD which is also the largest in this radiology center. In addition we know that the DAP is proportional to the dose and the surface. Note that the DRL in ESD is lower in the CHR of San-Pédro than the one in HG Bangolo, but the DAP in CHR San-Pédro (16.23 cGy·cm<sup>2</sup>) is higher than the one obtained at HG Bangolo (15.2 cGy·cm<sup>2</sup>). It is therefore clear that the area of exposure of patients is greater at the CHR of San-Pédro than HG of Bangolo. Operators should properly manipulate the tube diaphragm at the CHR San-Pédro to avoid unnecessary patient exposure to the X-ray beam. We obtained, for all the centers of our study, for the examination of the frontal thorax (PA), the DRL in ESD equal to 0.40 mGy (**Table 2**). The comparison of this value with that obtained in Abidjan for five (5) centers (0.22 mGy) [3], indicates that the DRL in ESD in west of Côte d'Ivoire is larger than that obtained in Abidjan in the south of the same country (**Figure 5**). An explanation for this result comes from the radiological parameters. The average voltage used in Abidjan (104 kV) is greater than the average voltage used in western Côte d'Ivoire (101.6 kV) (**Figure 6**) and the average electrical charge used in Abidjan (4.55 mAs) is smaller than that used in western Côte d'Ivoire (6 mAs) (**Figure 7**). The higher the voltage and the lower the electrical charge, the dose at the entrance is low. We also observe for DRL in DAP that the value obtained in Abidjan (53.26 cGy·cm<sup>2</sup>) (**Table 2** and **Figure 8**) is lower than that obtained in our study in western Côte d'Ivoire (54.85 cGy·cm<sup>2</sup>). The explanation comes from the fact that the DRL in ESD is weaker in Abidjan than in our study. By comparing the DRL in ESD from our study, obtained in the West of the Côte d'Ivoire to those obtained by the Institute for Radiation Protection and Nuclear Safety (IRNS) in France, the IAEA and other countries (**Figure 9**, **Figure 10**) we find

that our value is equal to that obtained in Nigeria and by the IAEA, close to those obtained in Iran and Cameroon. However it is larger than those obtained by the IRNS and the other countries. We can reduce the DRL in ESD of our centers of study, if the operators of medical imagery increase the tension more and reduce the charge. The FSR recommends a voltage range of (115 - 140) kV with a tendency to increase the voltage and electrical charge range (1.5 - 3) mAs with a tendency to reduce the charge [21]. The comparison of DRL in DAP of our study (54.85 cGy·cm<sup>2</sup>) with DRL in DAP obtained by the IRNS and other countries, (**Figure 11**), shows us that our value is greater. It is therefore necessary to take corrective measures by reducing the ESD and the area of exposure of the patients in the rooms of our study for the examination of the frontal chest.

## 5. Conclusions

We were able to achieve our goal of determining the DRL for ESD and DAP in western Côte d'Ivoire, for the postero-anterior frontal chest examination. The values that we obtained are for the DRL, in ESD 0.40 mGy and for the DRL in DAP, 54.85 cGy·cm<sup>2</sup>. The DRL values obtained for each of the sites in our study are different, which again justifies the need for the establishment of regional and national DRL. This disparity of values is justified by the choice of the radiological parameters by the technicians in the different rooms: voltage and electrical charges but also by the poor focusing of the beam. We also noted the importance of filtration in reducing the dose at the patient's entrance. Our DRL value in De is equal to that of the IAEA but greater than that of Abidjan and those of many countries such as the United Kingdom, Ghana and France. So there are efforts to be made in the rooms of our study to optimize the dose to patients. This involves the appropriate choice of voltage and electrical charge in accordance with IRNS recommendations and also by the equipment and a total equivalent filtration of 3 mm Al.

The value of DRL of DAP obtained in our study in western Côte d'Ivoire for the examination of the frontal chest (54.85 cG·cm<sup>2</sup>) is greater than those obtained in Abidjan and in several countries. It is therefore necessary not only to reduce the ESD but also to use the diaphragm of the tube to expose just the part of the patient's body to examine.

## Acknowledgements

The authors would like to express their gratitude to the Director of the National Public Health Laboratory (NPHL) and the staff of the (NPHL) for their availability and their DAPmeter available to us. The authors send their thanks to the Directors General of the three health establishments for having accepted to participate in this campaign.

## Conflicts of interest

The authors declare that they have no conflict of interest.

## References

- [1] IRSN PRP-HOM (2014) Analyse des données relatives à la mise à jour des niveaux de référence diagnostiques en radiologie et en médecine nucléaire. Bilan 2011-2012. Rapport parut en 2014.
- [2] Autorité de Sûreté Nucléaire (ASN) France (2013) Recueil de textes réglementaires relatifs à la radioprotection. Publié le 22/08/2013.
- [3] Konaté, I., Monnehan, G., Gogon, D., Koua, A. and Dali, T. (2017) Détermination des Niveaux de Référence Diagnostiques en radiologie thoracique à Abidjan. *Journal Africain d'Imagerie Médicale*, **9**, 1-6.
- [4] Konaté, I., Monnehan, G., Gogon, D., Kezo, C., Dali, T., Koua, A. and Koudou, D. (2017) Diagnostic Reference Level in Lumbar Radiography in Abidjan, Côte d'Ivoire. *The International Journal of Engineering and Science*, **6**, 31-35.  
<https://doi.org/10.9790/1813-0602023135>
- [5] Monnehan, G., Anouan, K., Onoma, D., Yao, K., Kouadio, L., Koua, A. and Dali, T. (2009) Détermination des Niveaux de Référence Diagnostiques en Côte d'Ivoire: Cas de la radiographie du thorax de face et de l'abdomen sans préparation (ASP) de face chez l'adulte dans le district d'Abidjan et dans la région du sud comoé. *Revue Internationale des Sciences et Technologie*, **14**, 45-53.
- [6] Journal Officiel (1967) Article 4D 497 du Décret n 67-321 du 21 juillet 1967, portant codification des dispositions réglementaires prises pour application du titre VI "hygiène et sécurité service médical" de la loi n 64-290 du 1er Aout 1964, portant code du travail 9 juillet 1968, Côte d'Ivoire.
- [7] Institut de Radioprotection et de Sûreté Nucléaire (IRSN) (2016) Analyse des données relatives à la mise à jour des niveaux de référence diagnostiques en radiologie et en nucléaire. Bilan 2013-2015. Rapport de mission 2016.
- [8] PTW. User manual diasoft (2014) Version 5.2. D154.131.O/7. Manuel d'instructions 2014.
- [9] Leclot, H. (2016) La métrologie des niveaux de dose dans les pratiques radiodiagnostiques. <http://www.bivi.metrologie.afnor.org>
- [10] Glossaire-Statistica, Centile (2016).  
<http://www.statsoft.fr/concepts6statistiques/glossaire/C/centile>
- [11] Mazerolle. Moyenne arithmétique (2012) Notes de cours.
- [12] Asadinezhad, M. and Toosi, M. (2008) Doses to Patients in Some Routine Diagnostic X-Ray Examinations in Iran/Proposed the First Iranian Diagnostic Reference Levels. *Radiation Protection Dosimetry*, **132**, 409-414.  
<https://doi.org/10.1093/rpd/ncn308>
- [13] Homolka, P. (2009) Center for Biomedical Engineering and Physics Medical University of Vienna, Austria, IAEA. Diagnostic Reference Levels (Guidance Levels). IAEA Training Course on Medical Physics in Diagnostic Radiology. Trieste, Italy May 11-15 2009.
- [14] Hart, D., Hillier, M. and Shrimpton, P. (2012) Doses to Patients from, Radiographic and Fluoroscopic X-Ray Imaging Procedures in the UK-2010. Review HPA-CRCE-034, R June 2012, 81 p.
- [15] Obed, R., Ademola, A., Adewoyin, K. and Akunade, O. (2007) Doses to Patients in Routine X-Ray Examinations of Chest, Skull, Abdomen and Pelvis in Nine Selected Hospitals in Nigeria. *Research Journal of Medical Sciences*, **1**, 209-214.
- [16] Odette, N., Jean, Y., Roméo, T., Alain, G. and Fai, C. (2015) Niveaux de référence diagnostiques en radiographie thoracique à Yaoundé. *Journal Africain de l'imagerie*

*Médicale*, **3**, 152-162.

- [17] Suliman, I.I., Abbas, N. and Habbani, F. (2007) Entrance Surface Doses to Patients Undergoing Selected Diagnostic X-Ray Examinations in Sudan. *Radiation Protection Dosimetry*, **123**, 209-214. <https://doi.org/10.1093/rpd/ncl137>
- [18] Muhogora, W., Ahmed, N., Almosabihi, A., Alsuwaidi, J., Beganovic, A., Cijraj-Bjéac, O., Shandorf, C., Rehani, M., Ramanazndraibe, M., Mukwadag, M. and Rouzitalab, J. (2008) Patient Doses in Radiographic Examinations in 12 Countries in Asia, Africa and Eastern Europe: Initial Results from IAEA Projects. *American Journal of Roentgenology*, **190**, 1453-1461. <https://doi.org/10.2214/AJR.07.3039>
- [19] Bundesamt für Strahlenschutz (2018) The Updated Diagnostic and Interventional X-Ray Examinations. Germany Federal Gazette. <http://www.bfs.de/EN/topics>
- [20] Office fédéral de la santé publique, Berne, Suisse Directive R-06-04 (2011) Niveaux de référence diagnostiques (NRD) en radiologie par projection 2011. Division radioprotection. <http://www.sfr-rad.ch>
- [21] Société Française de radiologie (SFR) (2014) Guide des procédures radiologiques. Critère de qualité et d'optimisation. 26/03/2014. Rapport SFR/OPRI.
- [22] Foulquier, J. (2010) Éléments technologiques permettant de réduire la dose en radiologie conventionnelle et numérique. *Journal de Radiologie*, **91**, 1225-1230. [https://doi.org/10.1016/S0221-0363\(10\)70178-5](https://doi.org/10.1016/S0221-0363(10)70178-5)

# Evaluation of Dosimetric Performance and Global Uncertainty of the Harshaw 6600 Plus System Used to Staff Monitoring in Côte d'Ivoire

Omer Kouakou<sup>1\*</sup>, Georges Alain Monnehan<sup>1,2</sup>, Gogon B. D. L. Huberson<sup>1</sup>

<sup>1</sup>Laboratoire de physique nucléaire et radioprotection, Unité de Formation et Recherche, Sciences des Structures de la Matière et Technologie, Université Félix Houphouët Boigny, Abidjan, Cote d'Ivoire

<sup>2</sup>Laboratoire National de la Santé Publique; Ministère de la Santé et de l'Hygiène Publique, Abidjan, Cote d'Ivoire  
Email: \*ladjuepe@gmail.com

**How to cite this paper:** Kouakou, O., Monnehan, G.A. and Huberson, G.B.D.L. (2019) Evaluation of Dosimetric Performance and Global Uncertainty of the Harshaw 6600 Plus System Used to Staff Monitoring in Côte d'Ivoire. *World Journal of Nuclear Science and Technology*, 9, 159-173.

<https://doi.org/10.4236/wjnst.2019.94012>

**Received:** July 19, 2019

**Accepted:** September 8, 2019

**Published:** September 11, 2019

Copyright © 2019 by author(s) and Scientific Research Publishing Inc.

This work is licensed under the Creative Commons Attribution International License (CC BY 4.0).

<http://creativecommons.org/licenses/by/4.0/>



Open Access

## Abstract

The objective of this work is to check the dosimetric performances of the TLD-100 as stated by the manufacturer as well as the technical standards of radiation protection. The purpose of the performance audit is to assess the inhomogeneity of TLD sensitivity, repeatability and reproducibility, linearity, energy dependence, angular dependence, and fading. All tests were performed under the conditions of ambient temperature and relative humidity recommended by the manufacturer. We began the study by calibrating the Harshaw 6600 Plus, and checking its performance. The TLD-100 performance verification results were all acceptable and in accordance with the manufacturer's advertised values and the radiation protection technical standards. However the performance of the TLD-100 that we have evaluated may have some limitations; these limits, which are sources of uncertainty, have been taken into account in this work by evaluating the overall uncertainty of the Hp (10) dose in the uncertainty range 9.45% to 15.80% by simple formulas. The TLD-100 personal dosimeters and the 6600 Plus reader system indicate that the calculated values of the overall uncertainty Hp (10) are well below the allowable values of 21% to 42% suggested for personal dosimetry services. The obtained data encourage the use of the system for the routine evaluation of the external exposure of workers under ionizing radiation in our laboratory.

## Keywords

Overall Uncertainty, Dosimetric Performances, Tests, Dosimetry Services, External Exposure of Workers

## 1. Introduction

Individual radiological monitoring of workers under ionizing radiation is a regulatory requirement of a radiological protection program [1] that respects the optimization principle [2] [3]. Since 1999, the National Laboratory for Public Health (LNSP), created by decree n° 91-605 of October 09, 1991, through its Subdivision of Protection against Ionizing Radiation (SDPRI), monitors workers' radiation exposure in Ivory Coast [4] using the thermoluminescence technique. The new Harshaw 6600 Plus model dosimetry system offered in 2014 by the International Atomic Energy Agency (IAEA) is based on the phenomenon of thermoluminescence. For accredited dosimetry laboratories, ISO/IEC 17025:2005 [5] (E) requires an acceptance procedure for any new equipment. Considering that, the creation of the new regulatory authority for radiation protection and nuclear safety (ARSN) through the IVC 6012 project entitled "Establishment of a Secondary Calibration Laboratory and Quality Management" has decided to work according to a quality management approach taking into account the evaluation of the performance of its measurement system [6]. Before the creation of the Laboratory Calibration Calibration and its assessment, this present work carried out under different conditions of irradiation, through dosimetric tests such as the inhomogeneity of the sensitivity of the TLD, the repeatability and the reproducibility, the linearity, energy dependence, angular dependence and fading, involves a quality approach to check the dosimetric performance of TLD-100 as announced by the manufacturer. The sources of erroneous estimation in the evaluation of the measurement of the Hp (10) doses and the deviations of the operating parameters of the reader [7] have been exploited to evaluate the overall uncertainty of the TLD system for the surveillance of people exposed to ionizing radiation in Côte d'Ivoire.

## 2. Materials and Methods

The Harshaw 6600 Plus dosimetry system developed and produced by Thermo Fisher Scientific (TFS) is composed of thermoluminescent dosimeters (TLDs) in LiF: Mg, Ti, and a reader.

### 2.1. Materials

#### 2.1.1. Description of TLD-100 Samples

The dosimeter consists of four chips LiF: Mg, Ti mounted in Teflon on an aluminum card and placed in a plastic holder. The carrier contains a unique filter for each copper, acrylonitrile-butadiene-styrene, Mylar and tin chip. These chips have the property of storing energy received during irradiation and returning it after heating in the form of light. Two of these pellets of size  $3.2 \times 3.2 \times 0.38 \text{ mm}^3$  and  $3.2 \times 3.2 \times 0.15 \text{ mm}^3$  in the plate make it possible to evaluate respectively equivalent doses at the level of the skin Hp (0.07) and at the level of the body Hp (10). Each card has a separate number associated with a barcode allowing for faster backup during playback.

### 2.1.2. Description of the Reader

The reader of **Figure 1** is composed of electronic circuits. During the reading, periodic checks of the intensity of the internal source, the reference light (RL) and the noise of the two photomultiplier tubes (PMT) are done at the beginning and at the end of each new dosimeter group. The procedure used to read the cards is to select the heating parameter using the Winrem analysis software. The heating profile is a preheat to 50°C and a linear heating rate of 25°C/sec up to 300°C, for a total time of 13.3 seconds.

## 2.2. Methods

### 2.2.1. Performance Ratings Dosimetry TLD-100

The reader is calibrated in physical unit (mSv) by irradiating the dosimeters “gold” of calibrations at the Secondary Laboratory of Dosimetry Calibration (LSED) of the Nuclear Research Center of Algiers (CRNA, Algeria), compared to Hp (10) and Hp (0.07). The reader calibration factor (RCF) and the factors that correct the different sensitivities of the dosimeters (ECC) have been determined. We collected data from the CCT database. Then, in **Figure 2**, we drew the frequency curve of the cards of each operational quantity Hp (10) and Hp (0.07) in positions (ii) and (iii) of the various pellets as a function of the individual ECCs in order to determine the average of the distribution and the proportion of cards that presents a recurrent ECC.

We found a normal distribution shifted to the left of which 5% of the cards for the chip in Hp (10) and 4.5% for the pellet in Hp (0.07) have after the calibration of the reader a recurring value of 0, Mean values and standard deviations of the shifted normal distribution are  $0.94 \pm 0.09$  for Hp (10) and  $0.96 \pm 0.1$  for hp (0.07), respectively. From the analysis we have chosen the cards whose ECC were outside the average value and the recurrent value of the distribution that is to say out of range (0.85 - 1.03). These are the chosen maps that have been experimentally characterized. With the exception of the inhomogeneity of batches of



**Figure 1.** The reader Harshaw 6600 Plus.

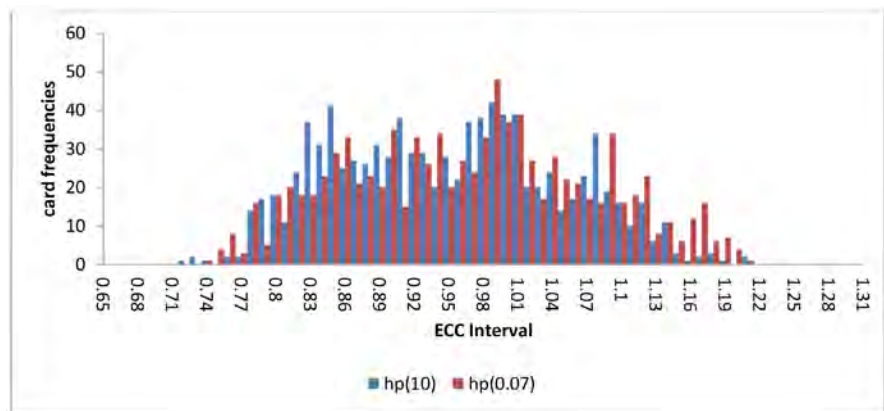


**Figure 2.** ECC distribution of the total number of cards available at S /DPRI.

dosimeters, Repeatability and Reproducibility carried out using strontium source internal to the reader; all the other irradiations were carried out in different SSDLs during training courses financed by the IAEA. After all the irradiations, the dosimeters with similar fadings [8] are conveyed to be read by the reader.

#### 1) Linearity

We exposed to Cs-137 12 batches of dosimeters; each batch is composed of 4 TLD dosimeters at doses ranging from 0.03 to 15 mSv. Exposure time ranges from 1.69 minutes to 20.34 minutes.

#### 2) Inhomogeneity of Batches of Dosimeters

For these measurements, we have, as far as possible, used TLDs from the same batch of our choice. We have irradiated 100 TLD dosimeters of the same batch at an identical dose of 1 mSv from a beam strontium 90 Sr/Y.

#### 3) Repeatability and Reproducibility

Ten (10) exposures of ten (10) 90 Sr/Y TLD-100 dosimeters were performed under the same conditions. The reference dose is of the order of 1000 gU or 10.83 mSv for an exposure time of 101.7 s per card. The mean value, standard deviation, and coefficients of variation and responses were determined in **Table 1** and **Table 2** for each of the ten (10) irradiations and each of the ten (10) dosimeters.

#### 4) Angular Dependence

The irradiations were carried out in accordance with the reference standards of the national center for radiological protection with a calibrated beam of Cs-137 (OB6 irradiator). We exposed to 2.56 mSv which corresponds to the exposure time of 16 min a series of eleven batches of dosimeter each consisting of two TL cards irradiated in the same reference position fixed by the lasers. Each lot is exposed in a clearly defined direction. TLD positions for all measures were identical. After each rotation, the geometric center of the detectors is returned. The rotation of the set (phantom + dosimeter) in the clockwise direction assumed to be the positive values of the angles (0°, 15°, 30°, 45°, 60°, 75°) and counterclockwise

**Table 1.** Average ( $\bar{x}$ ), Standard deviation ( $\sigma$ ), Coefficient of variation (CV)%, Response for each irradiation.

Irradiation (Réproductibilité)	Average ( $\bar{x}$ )	Standard déviation ( $\sigma$ ) %	Coefficient of variation (CV)%	Response %
1	10.853	11	1.07	100
2	10.856	11	1.04	100
3	10.743	11	1.04	99
4	10.826	17	1.65	99
5	10.67	12	1.13	98
6	10.823	13	1.25	99
7	10.743	12	1.09	99
8	10.853	12	1.15	100
9	10.751	12	1.12	99
10	10.865	13	1.17	100

**Table 2.** Average ( $\bar{x}$ ), Standard deviation ( $\sigma$ ), Coefficient of variation (CV)%, Response for each dosimeter.

Dosimeter (Repetability)	Average ( $\bar{x}$ )	Standard deviation ( $\sigma$ )%	Coefficient of variation (CV)%	Response %
1	10.795	9	0.9	99
2	10.983	7	0.6	100
3	10.679	9	0.8	98
4	10.911	8	0.7	99
5	10.547	6	0.6	99
6	10.827	7	0.6	99
7	10.861	6	0.6	98
8	10.856	7	0.6	100
9	10.757	7	0.6	99
10	10.767	5	0.5	100

the negative values ( $0^\circ$ ,  $-15^\circ$ ,  $-30^\circ$ ,  $-45^\circ$ ,  $-60^\circ$ ,  $-75^\circ$ ).

##### 5) Energy Dependence

The irradiations were carried out in accordance with the reference standards of the Secondary Laboratory of Dosimetry Calibration (LSED) of the Nuclear Research Center of Algiers (CRNA, Algeria) using three types of beams. An OB6 type emitter emitting a  $^{137}\text{Cs}$  gamma beam, a philips radiography apparatus for the X ray beams, an ELDORADO 78 therapy unit for a  $^{60}\text{Co}$  beam.

##### 6) Thermal Fading

The irradiations were carried out in accordance with the reference standards of the CNESTEN laboratory (Morocco). To highlight the phenomenon of thermal fading, or loss of signal, twenty-four (24) dosimeters were positioned in groups of six (06) on a standardized ghost. They were irradiated with a source of

cs-137, which emits  $\gamma$ -rays of 662 keV at a dose of 5 mSv for 32 min. After irradiation, TLDs were stored under ambient temperature conditions (25°C). Batch readings of four (04) dosimeters were performed at variable times ranging from 24 hours immediately after irradiation to 180 days.

### 2.2.2. Assessments of Global Uncertainty

Two methods of formulating and calculating the overall uncertainty of the TLD system have been applied.

#### 1) Global Method

The first method, called global, is a posteriori estimation of the total uncertainty of the system. It defines two types of uncertainty: The type “A” and the type “B” [9]

Type A, called random involves uncertainties that can in fact be reduced by increasing the number of measurements.

Type B, called systematic is made up of uncertainties that cannot be reduced in number of repeated measures.

It is assumed that the variables to be taken into account follow a uniform or normal statistical distribution. In case the distribution is normal, the Type B uncertainty can be in the form of a standard deviation by dividing the half maximum difference measured by  $\sigma_i = \frac{\text{maximum measured half difference}}{3}$  [10]

where the maximum measured half difference of an amount  $X$  is calculated as follows: [10] where the maximum measured half difference of an amount  $X$  is calculated as follows:

$$\text{Maximum measured half difference} = \frac{\text{Max}(X) - \text{Min}(X)}{2}$$

The overall uncertainty is then:

$$U_{\text{total système}} = \sqrt{\sum U_A^2 + \sum U_B^2}$$

$$U_{\text{total système}} = \sqrt{\sum U_A^2 + \frac{1}{3} \sum \frac{\text{Max}(X) - \text{Min}(X)}{2}} \quad (1)$$

Or  $U_A$  and  $U_B$  are the uncertainties of type  $A$  and type  $B$ .

For the calculation of this formula, sources of type  $A$  uncertainties are:

- The Variation of Sensitivity Factors of the Dosimeters (ECC)
- Dosimetric variability (Repeatability and reproducibility of the response)

Sources of uncertainty type  $B$  are:

- The irradiation source 90 Sr/Y obtained by experience
- The calibration factor of the reader provided by laboratory of Algiers
- The electronic parameters of the reader provided by the specification sheet of the manufacturer [11].
- The nonlinearity obtained provides the specification sheet of the manufacturer or experimentally.

## 2) Quadratic Summation Method of Each Source of Uncertainty

From formula (2), the dose received by a dosimeter  $j$  is evaluated.

$$Hp(10)_j = \frac{Q_j * ECC_j}{RCF} \quad (2)$$

Or RCF is the calibration factor of the reader,  $ECC_j$  are the sensitivity factors relative to each dosimeter,  $Q_j$  is the apparent dose,  $Hp(10)$  are the actual dose in positions (ii) TLD cards

For the TLD dosimeter, the uncertainty was estimated from the quadratic propagation law of the uncertainties of equation [8].

$$\sigma_y = \sqrt{\sum_i^n \left( \frac{\partial f}{\partial x_i} \right) (\sigma_{x_i})^2} \quad (3)$$

This formula does not take into account the correlations between the different sources of uncertainty. Variables are assumed to be independent.

From Equation (2), it is possible to identify the different sources of uncertainty of the TLD measure. This gives an expression of the total uncertainty on the TLD measure presented in Equation (4).

$$\frac{\sigma_D}{D} = \sqrt{\sum_i^5 \left( \frac{\sigma_{ECC_i}}{ECC_i} \right)^2 + \left( \frac{\sigma_{RCF}}{RCF} \right)^2 + \left( \frac{\sigma_Q}{Q} \right)^2} \quad (4)$$

Uncertainty on reading  $\sigma_Q$ 

The term  $\sigma_Q$  corresponds to the uncertainty on the reading. The estimation of this term is mainly based on the results of the study of the characterization of the parameters of performance Equation III summarizes all the uncertainties in reading: It is mainly the most significant influencing factors that have been used to estimate the uncertainty in reading.

With  $j = \{\text{linearity, inhomogeneity, Repeatability and reproducibility, linearity, energy, angle}\}$

Or,

$$\frac{\sigma_Q}{Q} = \sqrt{\sum \sigma_j^2} \quad (5)$$

**Table 3** presents all distributions of uncertainties about reading.

Uncertainty on Ecc sensitivity of TLD  $\sigma_{ecc}$ :

$\sigma_{ecc}$ : corresponds to the uncertainty about the sensitivity of the TLD. It is given by the builder or experimentation by determining the standard deviation of the Ecc distribution.

Uncertainty about calibration:

$\sigma_{RCF}$  corresponds to the uncertainty on the calibration. This uncertainty was provided by Algeria's secondary calibration laboratory. It takes into account the intrinsic uncertainty and the standard deviation of the measurement performed on cesium-137.

**Table 3.** Distribution of all uncertainties on reading.

uncertainty (%)	Type	Distribution
$\sigma_{\text{linearity}}$	B	Normal
$\sigma_{\text{inhomogeneity}}$	A	Expérimental standard déviation of the mean
$\sigma_{\text{Repeatability et reproductibility}}$	A	Expérimental standard déviation of the highest average enters on repeatability and reproducibility
$\sigma_{\text{energy}}$	B	Normal
$\sigma_{\text{angle}}$	B	Normal
$\sigma_{\text{fading}}$	B	Normal

Overall uncertainty about the dose measurement of the TLD.

Finally, the total uncertainty on the TLD measure was calculated from the quadratic summation method on the over the low dose range.

### 3. Results and Discussions

#### 3.1. Performance Ratings Dosimetry TLD-100

##### 3.1.1. Linearity

**Figure 3** describes the evolution of the relative response of TLD dosimeters as a function of the dose equivalent Hp (10). The results were evaluated in terms of Hp (10). The upper line of the curve represents the maximum values of the response relative to the true value and the lower line the minimum values based on the experimental measurements, it is found that most of the results are located inside the trumpet curves. However, many dosimeters are unable to accurately measure in the low dose region. In the low dose range of 0.1 mSv to 10 mSv, the highest difference between the dose delivered and that measured is 27%. The calculated uncertainty of 4.5% is below that of the manufacturer. This confirms the common behavior of dosimeters used for occupational exposure monitoring. In the range of doses studied, TLDs respond to IAEA recommendations [12] on linearity. Therefore, it can be concluded that its linearity is sufficient for our use.

##### 3.1.2. Inhomogeneity of Batches of Dosimeters

**Figure 4** shows the results in the form of dose distributions. The maximum and minimum doses are respectively 1.36 mSv and 1.10 mSv. These values allow us to affirm that some dosimeters receive more dose and others less in relation to the value of exposure. Nevertheless, there is a flat profile, the values are distributed around the average readings of the order of 1.16 mSv. The calculation shows a standard deviation of the average of the order 6.7% on the responses of dosimeters of the same batch irradiated under the same conditions. On the other hand all the measured values are beyond the reference value. Standard [13] requires that the limit variation of the maximum and minimum dose relative to the mean value must be less than 30%. According to the manufacturer, this significant variation of 30% [11] over the entire population of dosimeters chosen is due to the physical mass of the pellets (manufacture). From these series of measurements,

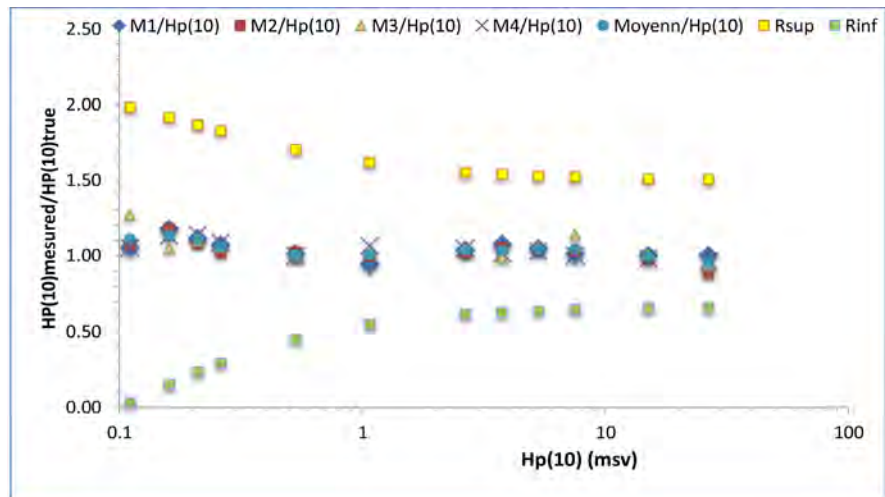


Figure 3. Linearity test according to IAEA recommendations.

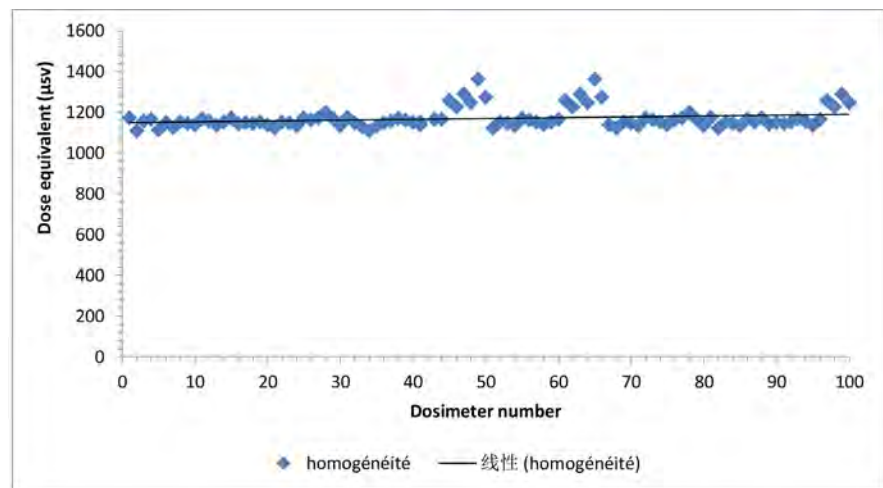


Figure 4. Inhomogeneity test.

we found a value of 22% which leads us to conclude that the batches of dosimeters used have a good homogeneity and a good stability for evaluation of the doses of routines of the workers exposed to the ionizing radiations.

### 3.1.3. Repeatability and Reproducibility

The repeatability or coefficient of variation is calculated by realizing the ratio of the standard deviation to the average of the measurements. The reproducibility of each irradiation (different dosimeters) is between 98% - 100%. These high values are considered good because the system manages to distinguish between dosimeters. The repeatability of each dosimeter is similar only by reasoning on the coefficient of variation for each measurement repeated on the same map it could be said that sometimes happens or the source  $^{90}\text{Sr}/\text{Y}$  still does not put the same dose in the sensitive volume of the tablet when it always carries out the same measurement process because we observe a slight variation of 0.5% to 0.9% or a margin of error of 0.4%.

For each of the 10 irradiations the values obtained are ranged from 1.71% - 2.07%.

For each of the 10 dosimeters the values obtained are ranked from 1.02% - 1.52%.

The coefficients of variation found at each irradiation and each map are below 2% for all exposures. These values obtained are in line with that of the manufacturer and that of the standard [14] which suggests that the coefficient of variation should not exceed  $\pm 5\%$ . The experimental standard deviation of the highest average of 4% between repeatability and reproducibility was taken as uncertainty.

#### 3.1.4. Angular Dependence

**Figure 5** shows the responses of the average dose of each lot of normalized dosimeter to the normal incidence value (reference angle). The angles correspond to each measurement point (positioning of the dosimeter). This was evaluated in terms of Hp dose (10, q) by rotating the dosimeter-phantom assembly about the vertical axis perpendicular to the direction of incident radiation. We find that the response varies depending on the irradiation angle. The response is maximum at normal incidence but decreases as the ghost rotates. Angles between  $15^\circ$  and  $60^\circ$  clockwise and counterclockwise respectively have a relative error range of [4% - 12.7%] to [4% - 19.4%]. The origin of these considerations could be explained by the fact that, the dosimeter and its case, are not necessarily exposed to direct beams. However, the maximum difference of 12.7% and 19.4% observed between responses of two-way TL measurements satisfies the requirements of ISO 4037-3 [15] which states that the difference between responses should not exceed 30%. Further, according to [14] the relative response due to an average energy greater than 65 Kev of the photon radiation and the angle of incidence must be in the range of  $-29\%$  to  $67\%$ . Our measurement results are satisfactory. The dosimeters are usable in the range from 00 to 600. However the detection anisotropy becomes more and more significant from  $\pm 75^\circ$ , where the maximum relative error varies from 62% to 65.5%. From this inclination the dosimeters do not respond easily.

#### 3.1.5. Energy Dependence

**Figure 6** shows the ratio of the reading average of four dosimeters and the true conventional value as a function of the photon energy for the Hp (10) patch at angle of incidence. The responses have been normalized to that of colbat 60. The normal incidence shows that the variation of the photon energy response for case 8814 in the range of 20 keV to 1250 keV is  $-50\%$  to  $+43\%$ . Generally, a good sensitivity of low energy X-rays between 20 and 250 keV is observed, however, the energy dependence is observed for these same x-ray beams or the relative response is between 0.97 and 1.47 compared to that of cesium (662 KeV) and cobalt (1250 Kev). This large difference in response is probably due to the dosimetric system which is not calibrated on X-ray and which does not use an

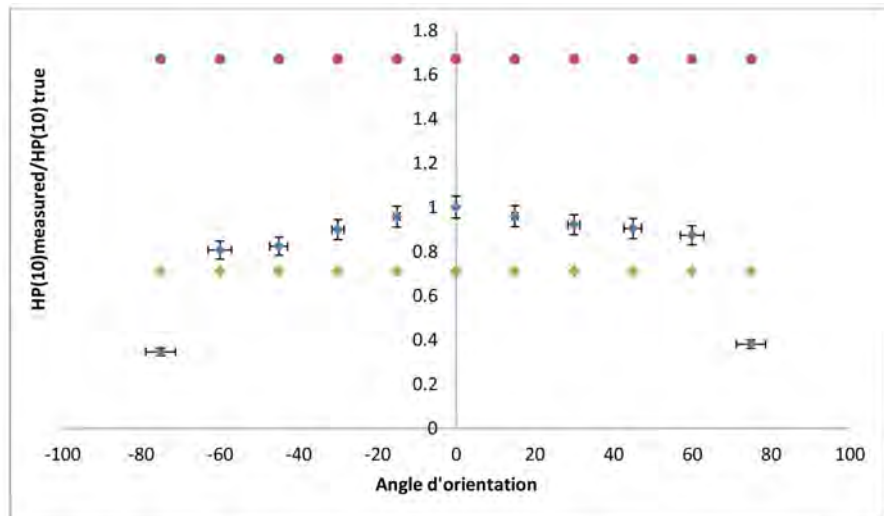


**Figure 5.** Response as a function of the angle of incidence (positive and negative) of the photons for the Cs-137 source. Values are normalized to 0° reference angle.

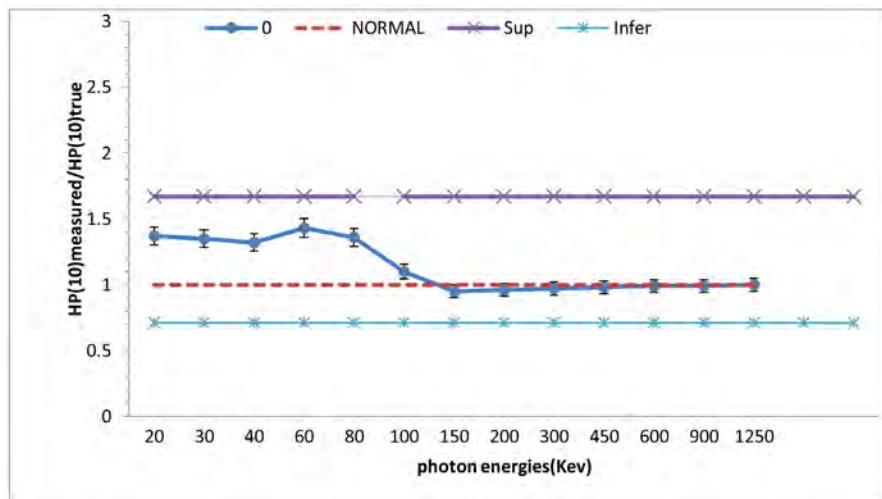


**Figure 6.** The ratio of the reading average of four dosimeters and the true conventional value as a function of the photon energy for the patch Hp (10) at 0° incidence angle. The answers have been normalized to that of colbat 60.

appropriate dose algorithm incorporating the X-ray beam qualities for the evaluation of Hp (10) [16] An optimal operating value of the response is found at 80 keV. Nevertheless the relative response of photon energies to the normal incidence compared to the manufacturer [10] and the recommendations of [12] is satisfactory.

### 3.1.6. Thermal Fading

**Figure 7** shows the evolution of the actual situation of fading according to the number of days of storage. Each graph of the relative response represents the average reading value of (04) dosimeters.

The signal of the first reading, 24 hours after irradiation, taken as reference is designated 100% of the luminescence. It is found that the greatest variation

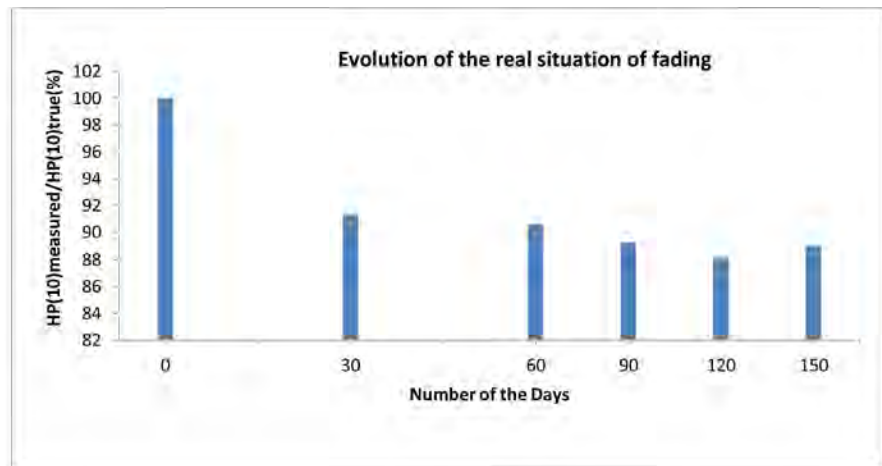


**Figure 7.** Relative response of the dosimeters as a function of the number of days of storage at room temperature.

occurs during the first 30 days after storage. After 30 days, the fading changes become less progressive, and can reach a correction factor so the average is 10% - 12% within 90 days to 150 days. What is very small compared to the characteristics of the manufacturer's material TLD-100 [11]. A significant variation in thermoluminescence was not observed in the 150 days of post-irradiation storage. These measurement results compared to that of the manufacturer and those of [17] [18] show satisfaction.

### 3.2. Assessments of Global Uncertainty

**Table 4** and **Table 5** show the results of the uncertainties that have been calculated and used in this work.

With regard to **Table 4** and **Table 5**, the uncertainties supposed to be much smaller are the sources of irradiations and the electronic components of the reader since the sources are well calibrated in accordance with the primary standards and the electronic components drift less.

The highest type A uncertainty is the variation in ECCs. This can be reduced by increasing the number of cards to be calibrated. The main source of type B uncertainty is the energy and angle dependency. The overall uncertainty calculated by the two approaches is in the range of 9, 45% to 15%, 80%. These values found in our current work are less than 21% and 42%, values recommended respectively by the ICRP [17] and RSG1.3 [18].

## 4. Conclusion

This work has assessed several parameters, the inhomogeneity of TLD sensitivity, repeatability and reproducibility, linearity, energy dependence, angular dependence and fading as part of our technical quality assurance approach proposed by the laboratory from the ARSN. This assessment made it possible to check the dosimetric performances of the TLD-100 as announced by the manufacturer and the technical standards of radiation protection. We then showed

**Table 4.** Assessment of uncertainty from the global method.

Source of uncertainty	Type A	Type B	
Variation of ECC	9%		
Irradiation source			0.4%
Reader		Reference light	1.0%
		High tension	0.005%
		Heating temperature	–
		PMT electronic noise	–
		linearity	1%
		Reader Calibration Factor	2.5%
Total type	9%		
Total system	9.45%		

**Table 5.** Assessment of uncertainty from the quadratic method.

Source of uncertainty	Type of distribution	Number of TLDs	Uncertainty value Hp (10) (%)
Reader Calibration Factor	-	24	2.5
Inhomogeneity of cards	Gaussienne (A)	100	6,7
Repeatability and reproducibility	Gaussienne (A)	10	4
Repeatability of ECC	Gaussienne (A)	187	9
Linearity	Gaussienne (B)	48	4.5
Angular dependence	Gaussienne (B)	24	10
Energy dependence	Gaussienne (B)	52	8
Fading	Gaussienne B)	24	2
Total system			15.80

that the energy and angle dependency is the main source of uncertainty [19]. The overall uncertainty calculated in **Table 4** and **Table 5** demonstrates that the system complies with the ICRP recommendation on overall accuracy (*i.e.*, an uncertainty range of  $-33\%$  to  $+50\%$  for near-limit doses) and that specified by GSR1.3. Despite the different irradiation conditions, the dosimeters were found satisfactory for the evaluation of the external exposure of workers under ionizing radiation. This work will be refined after the establishment of the secondary calibration laboratory. We can subtract the contribution of natural background radiation and determine the limit of detection.

### Conflicts of Interest

The authors declare no conflicts of interest regarding the publication of this paper.

### References

- [1] International Commission on Radiological Protection (1990) Recommendations of

- the International Commission on Radiological Protection. Publication No. 60, Pergamon Press, Oxford and New York.
- [2] CIPR 26 (1977) Recommandations 1977 de la Commission Internationale de Protection Radiologique. Pergamon Press, Oxford.
  - [3] CIPR 60 (1993) Recommandations 1990 de la Commission Internationale de Protection Radiologique. Pergamon Press, Oxford.
  - [4] Arrêté n° 32/MSPS/MEFP du 17 février 1992 (1992) Fixant les modalités de contrôle des activités liées à l'utilisation de sources de rayonnements ionisants et de radioéléments artificiels.
  - [5] International Organization for Standardization and International Electrotechnical Commission (2005) Conformity Assessment—General Requirements for Bodies Operating Certification of Persons. ISO/IEC 17025. ISO.
  - [6] Agence Internationale de l'Energie Atomique (2010) Radiation Monitoring & Protection Services for IAEA Operations. Annual Technical Report, 16.
  - [7] Luo (2010) Long Term Study of Harshaw TLD LiF-LLD and Uncertainty. *Radiation Measurements*, **45**, 569-572. <https://doi.org/10.1016/j.radmeas.2009.11.004>
  - [8] Rizk and Vanhavere, F. (2016) A Study on the Uncertainty for the Routine Dosimetry Service at the Lebanese Atomic Energy Commission Using Harshaw 8814 Dosemeters. *Radiation Protection Dosimetry*, **170**, 168-172. <https://doi.org/10.1093/rpd/ncv426>
  - [9] Joint Committee for Guides in Metrology (2008) Evaluation of Measurement Data—Guide to the Expression of Uncertainty in Measurement. JCGM 100:2008, BIPM.
  - [10] International Electrotechnical Commission (2015) Radiation Protection Instrumentation, Determination of Uncertainty in Measurement. IEC Technical Report TR 62461. IEC.
  - [11] Bicron (2002) Model 6600 Automated TLD Reader with WinREMS™ Operator's Manual. Publication No. 6600-W-O-0602-005. Bicron, Saint-Gobain/Norton Industrial Ceramics Corporation, Solon.
  - [12] GSR Part 3 (Interim). International Atomic Energy Agency (2011) Radiation Protection and Safety of Radiation Sources: International Basic Safety Standards—Interim Edition. General Safety Requirements Part 3. IAEA Safety Standards Series IAEA.
  - [13] International Electrotechnical Commission, International Standard (1991) Thermoluminescence Dosimetry Systems for Personal and Environmental Monitoring. CEI IEC 61066, 1991-2012, IEC, Geneva.
  - [14] International Electrotechnical Commission (2012) Radiation Protection Instrumentation-Passive Integrating Dosimetry Systems for Environmental and Personal Monitoring Part 1: General Characteristics and Performance Requirements. IEC62387-1.
  - [15] International Organization for Standardization (1993) X and Gamma Reference Radiations for Calibrating Dosemeters and Dose Rate Meters and for Determining Their Response as a Function of Photon Energy. Part 3: Calibration of Area and Personal Dosemeters and the Measurement of Their Response as a Function of Energy and Angle of Incidence. ISO 4037-3. ISO, Geneva.
  - [16] Arib, M., Herrati, A., Dari, F., Ma, J. and Lounis-Mokrani, Z. (2014) Intercomparison 2013 on Measurements of the Personal Dose Equivalent  $h_p(10)$  in Photon Fields in the African Region. *Radiation Protection Dosimetry*, **163**, 276-283.

<https://doi.org/10.1093/rpd/ncu202>

- [17] Alves, J.G., Abrantes, J.N., Margo, O., Rangel, S. and Santos, L. (2006) Long-Term Stability of a TLD-Based Individual Monitoring System. *Radiation Protection Dosimetry*, **120**, 289-292. <https://doi.org/10.1093/rpd/nci520>
- [18] Schandof, C., Asiamah, A.D. and Anim-Sampong, S. (2002) Performance of Harshaw 6600 Thermoluminescent Dosimeter (TLD), Système for Personal Monitoring. *Journal of Applied Science and Technology*, **7**, 37-43.
- [19] Van Dijk, J.W.E. (2011) Developments in Uncertainty Analysis for Individual Monitoring. *Radiation Protection Dosimetry*, **144**, 56-61. <https://doi.org/10.1093/rpd/ncq426>

# Qualification of the ANET Code for Spallation Neutron Yield and Core Criticality in the KUCA ADS

Xenofontos Thalia<sup>1\*</sup>, Panayiota Savva<sup>1</sup>, Melpomeni Varvayanni<sup>1</sup>, Jacques Maillard<sup>1</sup>, Jorge Silva<sup>1</sup>, Marc-Thierry Jaekel<sup>2</sup>, Nicolas Catsaros<sup>1</sup>

<sup>1</sup>Institute of Nuclear and Radiological Sciences & Technology, Energy & Safety, National Centre for Scientific Research Demokritos, Aghia Paraskevi, Greece

<sup>2</sup>Laboratoire de Physique de l'École Normale Supérieure, CNRS, Paris, France

Email: \*thalia.xenofontos@ipta.demokritos.gr

**How to cite this paper:** Thalia, X., Savva, P., Varvayanni, M., Maillard, J., Silva, J., Jaekel, M.-T. and Catsaros, N. (2019) Qualification of the ANET Code for Spallation Neutron Yield and Core Criticality in the KUCA ADS. *World Journal of Nuclear Science and Technology*, 9, 174-181.  
<https://doi.org/10.4236/wjnst.2019.94013>

**Received:** August 5, 2019

**Accepted:** October 21, 2019

**Published:** October 24, 2019

Copyright © 2019 by author(s) and Scientific Research Publishing Inc.

This work is licensed under the Creative Commons Attribution International License (CC BY 4.0).

<http://creativecommons.org/licenses/by/4.0/>



Open Access

## Abstract

Innovative nuclear reactor concepts such as the Accelerator Driven Systems (ADSs) have imposed extra requirements of simulation capabilities on the existing stochastic neutronics codes. The combination of an accelerator and a nuclear reactor in the ADS requires the simulation of both subsystems for an integrated system analysis. Therefore, a need arises for more advanced simulation tools, able to cover the broad neutron energy spectrum involved in these systems. ANET (Advanced Neutronics with Evolution and Thermal hydraulic feedback) is an under development stochastic code for simulating conventional and hybrid nuclear reactors. Successive testing applications performed throughout the ANET development have been utilized to verify and validate the new code capabilities. In this context, the ANET reliability in simulating the spallation reaction and the corresponding neutron yield as well as computing the multiplication factor of an operating ADS are here examined. More specifically, three cores of the Kyoto University Critical Assembly (KUCA) facility in Japan were analyzed focusing on the spallation neutron yield and the neutron multiplication factor. The ANET-produced results are compared with independent results obtained using the stochastic codes MCNP6.1 and MCNPX. Satisfactory agreement is found between the codes, confirming thus ANET's capability to successfully estimate both the neutron yield of the spallation reaction and the  $k_{\text{eff}}$  of a realistic ADS.

## Keywords

Monte Carlo, Neutronics Analysis, Code Validation, Accelerator Driven Systems

## 1. Introduction

The Monte Carlo (MC) approach for reactor core analysis has steadily gained ground over the past decades due to the increased complexity of the reactor fuel and core configurations. Besides, new reactor concepts offering increased safety as well as solutions for waste management require detailed analysis with computational tools of enhanced capabilities. The Accelerator Driven System (ADS) constitutes an innovative reactor concept, since it is subcritical (*i.e.* safer) and can use fuel elements containing minor actinides as long-lived radioactive waste of conventional reactors, contributing thus to their optimum management via transmutation. The ADS simulation should comprise two combined parts, *i.e.* the one concerning the beam of deuterons or protons produced by an accelerator inducing the spallation reaction and the other concerning the nuclear reactor core. It arises that a code which can inherently deal with both ADS subsystems, *i.e.* a code comprising a high energy physics module and a neutronics component, would be required. The ANET development has been largely motivated by the above mentioned needs.

Until recently, the most common way to analyze ADSs was by simulating the spallation target and the sub-critical core using two different dedicated codes. Typical codes used for the spallation reaction simulation include FLUKA [1] [2] and MCNPX [3] [4] [5], while several neutronics codes are utilized for the neutronic/thermal-hydraulic subcritical core analysis, e.g. [6]. Only in a few cases [7] [8], effort has been made to analyze ADSs using a single code able to cover the broad energy neutrons spectrum involved in these systems.

The ANET development has been based on the open-source version of GEANT3.21 [9] which has been originally designed to analyze high energy physics (HEP) experiments. GEANT3.21 has been utilized as capable to simulate the passage of elementary particles through matter providing thus a tool for the analysis of the ADS accelerator/spallation target subsystem. At a first stage, the GEANT3.21 capability to be applied on nuclear reactor analysis was sought through the expansion of the treated energy spectrum to lower energies, so as to include the part involved in neutronics analysis and also through the incorporation of fission reactions [10] [11]. In the current ANET version, a bulk of sub-routines has been incorporated so that the computation of the neutron multiplication factor, the neutron flux and the reaction rates are treated strictly with the stochastic approach using the standard MC estimators [12]. ANET code is continuously developing targeting at an enhanced MC code which will be also capable of performing core isotopic evolution calculations for conventional and innovative reactors, being at the same time prepared to be coupled with thermal-hydraulic solvers. The ANET code performance on dynamic reactor core analysis was preliminarily tested [13] and proved very promising indicating the code capability to inherently provide a reasonable prediction for the core inventory evolution. Moreover in [14], the ANET preliminary results are presented for an ADS concept that can operate as a breeder reactor. The present work fo-

cuses to the steady state ANET applicability to ADSs and in particular to its ability to inherently simulate the spallation process and compute the resulting neutron yield as well as the neutron multiplication factor of an operating ADS.

## 2. The ANET Code

ANET's development efforts begun in the 1990s based on the open-source HEP code GEANT3.21, utilizing FORTRAN 90 as programming language. The main target for ANET's development is the creation of an enhanced computational tool in the field of reactor analysis, capable of simulating both GEN II/III reactors and ADSs. ANET is structured with the inherent capability of a) performing core evolution and fuel burnup calculations and b) simulating the spallation process in the ADS analysis, in addition to the classical static stochastic neutronics analysis. ANET is developed based on the estimation that numerous advanced codes should exist, for intercomparison and cross checking purposes. ANET also aspires to respond to the Nuclear Community's need for an advanced open source code.

The basis for ANET code was established following a fundamental GEANT3.21 modification, *i.e.* applicability extension for neutron energies below 20 MeV, which is the region of the neutron energy spectrum involved in fission nuclear reactors' analysis. During the particle tracking, the energy of the particle is checked and the particle is accordingly treated either by FLUKA or INCL/ABLA [15] for energies above 20 MeV or by standard ANET procedures (energy below 20 MeV). As a result, particles of a wide range of energies can be inherently simulated in ANET.

Concerning neutrons interactions, at this stage ANET includes elastic collision, capture and fission. For elastic collision, the energy dependent angular distribution is used, taking also into account the effect of temperature. The treatment of the inelastic scattering will be implemented in the code in the near future.

Point by point cross sections are pre-tabulated, using available nuclear data libraries for each nuclide-energy pair while  $S(\alpha, \beta)$  and probability tables can be utilized when required. For the current version of ANET the JEFF neutron library is available.

The current version of ANET code utilizes the three standard MC estimators for the neutron multiplication factor ( $k_{\text{eff}}$ ) calculation; that is the collision estimator, the absorption estimator and the track-length estimator are included. Regarding the simulation of neutron flux and reaction rates, the collision and the track-length estimators are implemented in ANET following the standard MC procedure. In addition, the ANET code has been successfully validated for its capability to reliably predict basic parameters of critical and subcritical reactor systems, namely the multiplication factor, neutron fluxes as well as neutron reaction rates, using international benchmarks and data from various installations [12].

### 3. Kyoto University Critical Assembly (KUCA)

The KUCA is located at the Kyoto University, Institute for Integrated Radiation and Nuclear Science (KURNS). The facility combines a subcritical assembly of solid - or water-moderated and reflected cores with the new fixed-field alternating gradient type accelerator installed in 2008. Thus pulsed protons of 100 MeV are injected onto the heavy metal target of Pb-Bi and the spallation neutrons produced are directed into the subcritical system. The latter is loaded with highly enriched uranium fuel while it is moderated and reflected with polyethylene or water [16]. At KUCA, cores A and B are moderated and reflected by polyethylene while core C is light water-moderated and reflected. At the normal operating state the three cores are operated at a very low power level (order of mW), while maximum power is 100 W.

For the present work, core A (**Figure 1(a)**) and particularly three variations of the main part of this core, *i.e.* Cases 1, 2 and 3 (**Figure 1(b)-(d)**) are selected. The normal fuel assembly in this core is represented as (F, 3/8”P36EU). It is composed of 36 fuel plates (unit cells) contained between two polyethylene blocks in an Al sheath. The Pb-Bi loaded fuel rod is consisted of 60 fuel plates, half of which contain Pb-Bi. At both rod boundaries polyethylene blocks exist. The aforementioned Al sheathing endues the above components. In the fuel area of the normal fuel assemblies a unit cell includes an enriched uranium fuel plate and two polyethylene plates. The Pb-Bi loaded fuel assemblies include two unit cells, both of them containing a highly-enriched uranium (HEU) fuel plate and a polyethylene or Pb-Bi plate. For the selected core configurations, all the control and safety rods are withdrawn. Precise descriptions of the fuel assemblies as well as the atom densities of the materials that compose the core elements, *i.e.* the HEU fuel plate, the polyethylene reflector, the polyethylene moderator, the aluminum sheath, the spallation target and the coating materials over Pb-Bi plate, are presented in detail in [16]. Regarding the accelerator, the main characteristics of the proton beam are 1 nA intensity, 20 Hz pulsed frequency, 100 ns pulsed width and 40 mm diameter spot size at the spallation target. A detailed description of the experiments that are conducted in the Kyoto University facility along with the relevant results can be found in [16].

### 4. Simulations

In the frame of the validation and verification of ANET's capability to fully analyse an operating ADS, *i.e.* simulate the proton beam, the spallation reaction on the target, the spallation-generated neutrons (*i.e.* the neutron yield), and finally compute the neutron multiplication factor  $k_{\text{eff}}$  of the subcritical core, the KUCA configurations 4, 5 and 6 were chosen. For this task, ANET results were compared to the results produced by the well-established stochastic neutronics codes MCNP6.1 [17] and MCNPX [18].

The core was modelled in a three-dimensional geometry by ANET and MCNP6.1 while the reference libraries for this task were JEFF3.1.2, ENDFBV-II

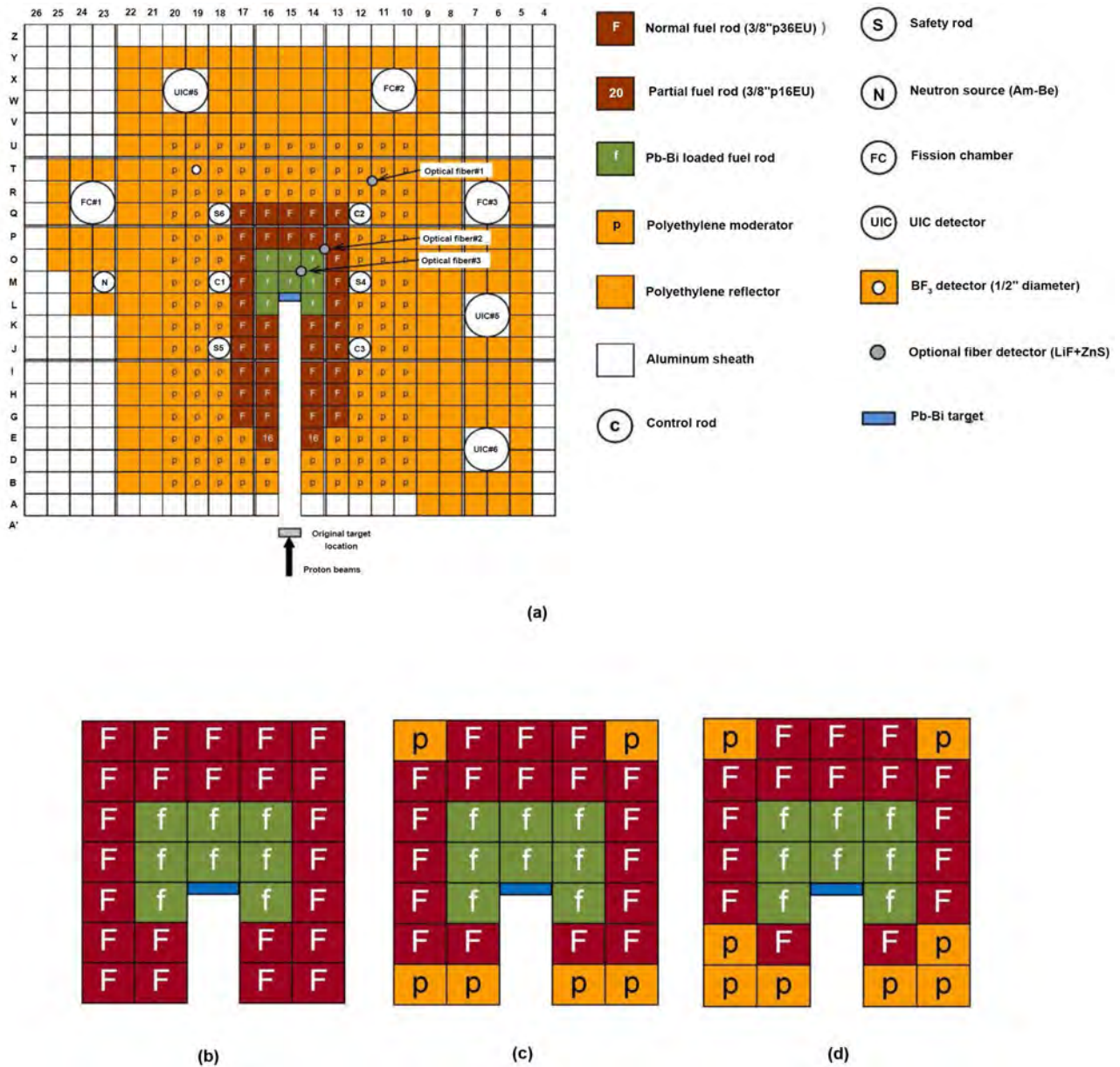


Figure 1. Top view of the KUCA A-core with 100 MeV protons. (b) Case 1. (c) Case 2. (d). Case 3.

and JENDL/HE-2007. MCNPX and the JENDL/HE-2007 library were employed for the simulation of the spallation procedure and the prediction of the neutron yield of the Pb-Bi target. ANET simulated the 100 MeV proton beam and the Pb-Bi target so as to produce the neutrons generated from spallation with the incorporated FLUKA module. The initial spatial and energetic distribution of the neutrons is the one derived from the spallation process. In ANET,  $2 \times 10^4$  cycles of  $3 \times 10^4$  particles were considered, which for the first cycle were protons while the neutrons generated from the spallation were stored and utilized for the second cycle. Subsequently, the standard MC treatment for the simulation cycles was applied. The neutron yield results for ANET are presented in Table 1 and are in very good agreement with the MCNPX results [19].

**Table 1.** Neutron yield computed by the ANET and MCNPX codes.

Code/Neutron Library	Neutron yield
ANET/JEFF3.1.2	$0.39 \pm 0.01$
MCNPX/JENDL/HE-2007	$0.38 \pm 0.01$

**Table 2.** Comparison between the results of  $k_{\text{eff}}$  by ANET and MCNP6.1 codes.

Code/Neutron Library	$k_{\text{eff}}$		
	Case 1	Case 2	Case 3
ANET/JEFF3.1.2	$0.95111 \pm 4.0\text{e-}04$	$0.90667 \pm 4.3\text{e-}04$	$0.89319 \pm 4.2\text{e-}04$
MCNP6.1/ENDFBV-II	$0.95784 \pm 4.0\text{e-}04$	$0.91355 \pm 4.0\text{e-}04$	$0.90006 \pm 4.0\text{e-}04$
MCNP6.1/ JENDL/HE-2007	$0.95409 \pm 1.1\text{e-}04$	$0.90996 \pm 1.0\text{e-}04$	$0.89641 \pm 1.0\text{e-}04$

The results concerning the  $k_{\text{eff}}$  including the value obtained by MCNP6.1 simulations performed in the KUCA laboratory [16] [20], are presented in **Table 2**. ANET vs MCNP results' discrepancies concerning  $k_{\text{eff}}$  are 673 pcm and 298 pcm for Case 1, 688 pcm and 329 pcm for Case 2, and 687 pcm and 322 pcm for Case 3 for MCNP/ENDFBV-II and MCNP/JENDL/HE-2007 respectively. In all cases, the ANET/MCNP discrepancies remain equivalent to, or lower than those found in typical benchmarks [21] and it is noticeable that ANET and MCNP6.1 results when using JENDL/HE-2007 are in better agreement compared to those obtained by MCNP6.1/ENDFBV-II. The intercomparison of MCNP6.1  $k_{\text{eff}}$  computations with ENDFBV-II and JENDL/HE-2007 reveal variations ranging from 359 pcm to 375 pcm. The  $k_{\text{eff}}$  simulations point out that the influence of the neutron library on the results should be further studied.

## 5. Conclusions & Future Work

Three core configurations of the KUCA system were fully modelled by ANET in order to perform criticality tests in an operating ADS. FLUKA was employed as a high energy physics simulator in ANET to perform the spallation simulation and compute the neutron yield while the  $k_{\text{eff}}$  was computed by utilizing exclusively the relevant procedures for the standard stochastic estimators incorporated in ANET. The results were compared with independent simulations conducted at the KUCA facility using MCNP6.1 and MCNPX. The comparison showed that ANET successfully simulates the neutron yield of the spallation process as well as the criticality of an ADS indicating thus that the development of this advanced stochastic neutronics code, targeting to analyze not only conventional but innovative nuclear fission reactors as well, is proceeding satisfactorily. Further, a key point to ANET's development has been the incorporation of new procedures that account for the assessment of the temporal changes in the fuel composition with very promising preliminary results [13]. This feature will also be validated by comparison with very recent measurement results of nuclear

transmutation of Minor Actinides (Np-237 and Am-241) obtained in KUCA [22].

## Acknowledgements

Authors would like to thank Dr Masao Yamanaka and Pr. Cheol Ho Pyeon from Institute for Integrated Radiation and Nuclear Science, Kyoto University 2, Osaka, Japan for their collaboration in the acquisition and exploitation of data from the KUCA facility.

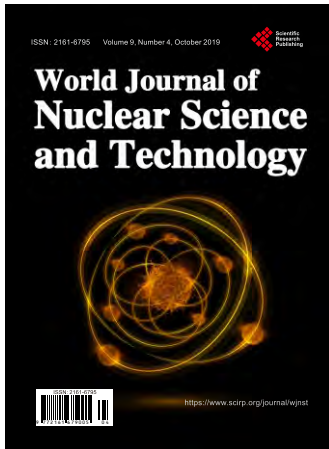
## Conflicts of Interest

The authors of this manuscript wish to declare that there is not any conflict of interest regarding this work.

## References

- [1] Ren, G., Li, W., Li, Y. and Zeng, M. (2013) Simulation for Radiation Field Caused by Beam Loss of C-ADS Injector II. *International Beam Instrumentation Conference*, Oxford, 16-19 September 2013, 489-491.
- [2] Mantha, V., Mohanty, A.K. and Satyamurthy, P. (2007) Thermal Hydraulic Studies of Spallation Target for One-Way Coupled Indian Accelerator Driven Systems with Low Energy Proton Beam. *Pramana—Journal of Physics*, **68**, 355-363. <https://doi.org/10.1007/s12043-007-0040-6>
- [3] Fegghi, S.A.H. and Gholamzadeh, Z. (2013) A MCNP Simulation Study of Neutronic Calculations of Spallation Targets. *Nuclear Technology and Radiation Protection*, **28**, 128-136.
- [4] Louis, H., Amin, E., Aziz, M. and Bashter, I. (2012) Studies on Production of Neutrons in the Spallation Reactions Using the Monte Carlo Code MCNPX. *Nuclear Science and Engineering*, **170**, 61-65. <https://doi.org/10.13182/NSE11-11>
- [5] Barros, G.P., Pereira, C., Veloso, M.A.F., Costa, A.L. and Reis, P.A.L. (2010) Neutron Production Evaluation from a ADS Target Utilizing the MCNPX 2.6.0 Code. *Brazilian Journal of Physics*, **40**, 414-418. <https://doi.org/10.1590/S0103-97332010000400010>
- [6] Meloni, P., Bandini, G. and Polidori, M. (2008) T/H and Transient Analyses to Confirm EFIT Preliminary Design. *Journal of Nuclear Materials*, **376**, 405-408. <https://doi.org/10.1016/j.jnucmat.2008.02.081>
- [7] Bungau, C., Barlow, R., Bungau, A. and Cywinski, R. (2009) Neutron Spallation Studies for an Accelerator Driven Subcritical Reactor. *23rd Particle Accelerator Conference*, Vancouver, 4-8 May 2009, 1351-1353.
- [8] Kadi, Y. and Carminati, F. (2001) Simulation of Accelerator-Driven Systems, Workshop on Hybrid Nuclear Systems for Energy Production, Utilisation of Actinides & Transmutation of Long-Lived Radioactive Waste, CERN, Geneva, Switzerland.
- [9] Brun, R., Hansroul, M. and Lassalle, J.C. (1994) GEANT3 User's Guide, CERN DD/EE/84-1. Computing and Networks Division, CERN.
- [10] Catsaros, N., Gaveau, B., Jaekel, M.-T., Maillard, J., Maurel, G., Savva, P., Silva, J., Varvayanni, M. and Zisis, Th. (2009) Criticality Qualification of a New Monte Carlo Code for Reactor Core Analysis. *Annals of Nuclear Energy*, **36**, 1689-1693. <https://doi.org/10.1016/j.anucene.2009.09.006>

- [11] Catsaros, N., Gaveau, B., Jaekel, M.-T., Maillard, J., Maurel, G., Savva, P., Silva, J. and Varvayanni, M. (2012) Building a Dynamic Code to Simulate New Reactor Concepts. *Nuclear Engineering and Design*, **246**, 41-48. <https://doi.org/10.1016/j.nucengdes.2011.10.015>
- [12] Xenofontos, T., Delipei, G.-K., Savva, P., Varvayanni, M., Maillard, J., Silva, J. and Catsaros, N. (2017) Testing the New Stochastic Neutronic Code ANET in Simulating Safety Important Parameters. *Annals of Nuclear Energy*, **103**, 85-96. <https://doi.org/10.1016/j.anucene.2017.01.012>
- [13] Xenofontos, T. (2018) Development of a Dynamic Stochastic Neutronics Code for the Analysis of Conventional and Hybrid Nuclear Reactors. PhD Thesis, Aristotle University of Thessaloniki (Greece) and Ecole Polytechnique de Paris, Paris.
- [14] Catsaros, N., Gaveau, B., Jaekel, M.-T., Jejcic, A., Maillard, J., Maurel, G., Savva, P., Silva, J., Varvayanni, M. and Xenofontos, T. (2013) Investigating the Breeding Capabilities of Hybrid Soliton Reactors. *Nuclear Engineering and Design*, **261**, 251-259. <https://doi.org/10.1016/j.nucengdes.2013.04.022>
- [15] Ferrari, A. and Sala, P.R. (1993) A New Model for Hadronic Interactions at Intermediate Energies for the FLUKA Code. *International Conference on Monte-Carlo Simulation in High-Energy and Nuclear Physics*, Florida, 22-26 February 1993, 277-288.
- [16] Pyeon, C.H., Yamanaka, M., Endoc, T., Fredrik, G., van Rooijend, W. and Chiba, G. (2017) Experimental Benchmarks of Kinetic Parameters in Accelerator-Driven System with 100 MeV Protons at Kyoto University Critical Assembly. *Annals of Nuclear Energy*, **105**, 346-354. <https://doi.org/10.1016/j.anucene.2017.03.030>
- [17] Goorley, J.T., James, M.R., Booth, T.E., Brown, F.B., Bull, J.S., Cox, L.J., Durkee, J.W., Elson, J.S., Fensin, M.L., Forster, R.A. III, Hendricks, J.S., Hughes, H.G. III, Johns, R.C., Kiedrowski, B.C., Martz, R.L., Mashnik, S.G., McKinney, G.W., Pelowitz, D.B., Prael, R.E., Sweezy, J.E., Waters, L.S., Wilcox, T. and Zukaitis, A.J. (2013) Initial MCNP6 Release Overview: MCNP6 Version 1.0. (LA-UR-13-22934).
- [18] (2002) MCNPX User's Manual, Version 2.4.0. Los Alamos, (LA-CP-02-408).
- [19] Pyeon, C.H., Nakano, H., Yamanaka, M., Yagi, T. and Misawa, T. (2015) Neutron Characteristics of Solid Targets in Accelerator Driven System with 100 MeV Protons at Kyoto University Critical Assembly. *Nuclear Technology*, **192**, 181-190. <https://doi.org/10.13182/NT14-111>
- [20] Pyeon, C.H. (2017) Experimental Benchmarks of Neutronics on Solid Pb-Bi in Accelerator-Driven System with 100 MeV Protons at Kyoto University Critical Assembly, Japan, KURRI, (KURRI-TR-447).
- [21] DICE (2001) International Handbook of Evaluated Criticality Safety Benchmark Experiments. NEA, OECD, (NEA/NSC/DOC(95)).
- [22] Pyeon, C.H. (2019) Unpublished Results, Personal Communication.



# World Journal of Nuclear Science and Technology (WJNST)

ISSN 2161-6795 (Print) ISSN 2161-6809 (Online)

<https://www.scirp.org/journal/wjnst>

*World Journal of Nuclear Science and Technology (WJNST)* is an international peer-reviewed, open access journal publishing in English original research studies, reviews in all aspects of nuclear science and technology and its applications. Symposia or workshop papers may be published as supplements.

## Editor-in-Chief

Prof. Andrzej Grzegorz Chmielewski

## Editorial Board

Dr. Abdullah Aydin  
Prof. Jiejun Cai  
Prof. Ahmet Cengiz  
Prof. Abdelmajid Choukri  
Prof. Snezana Dragovic  
Prof. Hardy Christian Ekberg  
Prof. Juan-Luis François  
Prof. Shilun Guo

Prof. Shaban Ramadan Mohamed Harb  
Prof. Xiaolin Hou  
Prof. Ning Liu  
Prof. Man Gyun Na  
Prof. Dragoslav Nikezic  
Dr. Rafael Rodríguez Pérez  
Prof. K. Indira Priyadarsini  
Prof. Massimo Rogante

Prof. Vitalii D. Rusov  
Dr. Chhanda Samanta  
Prof. Kune Y. Suh  
Prof. Wenxi Tian  
Dr. Heiko Timmers  
Prof. Marco Túllio Menna Barreto de Vilhena  
Dr. Jun Wang  
Dr. Leopoldo A. Pando Zayas

## Subject Coverage

This journal invites original research and review papers that address the following issues. Topics of interest include, but are not limited to:

- Fuel Cycle and Isotopes
- Global Nuclear Security Technology
- Nonreactor Nuclear Facilities
- Nuclear and Chemical Waste Management
- Nuclear and Particle Physics
- Nuclear Cardiology
- Nuclear Energy
- Nuclear Engineering and Design
- Nuclear Fusion
- Nuclear Instruments and Methods
- Nuclear Magnetic Resonance Spectroscopy
- Nuclear Materials
- Nuclear Medicine and Biology
- Nuclear Medicine and Molecular Imaging
- Nuclear Physics
- Nuclear Science and Techniques
- Nuclear Structural Engineering
- Nuclear Track Detection
- Nuclear Tracks and Radiation Measurements
- Radiation Applications and Instrumentation
- Radioanalytical and Nuclear Chemistry
- Reactor and Nuclear Systems
- Reactor Science and Technology

We are also interested in short papers (letters) that clearly address a specific problem, and short survey or position papers that sketch the results or problems on a specific topic. Authors of selected short papers would be invited to write a regular paper on the same topic for future issues of the WJNST.

## Notes for Intending Authors

Submitted papers should not have been previously published nor be currently under consideration for publication elsewhere. Paper submission will be handled electronically through the website. All papers are refereed through a peer review process. For more details about the submissions, please access the website.

## Website and E-mail

<https://www.scirp.org/journal/wjnst>

E-mail: [wjnst@scirp.org](mailto:wjnst@scirp.org)

